University of Alberta

One-step Oxidation of Ethylene to Acetic Acid using Hydrophobic Catalysts

by

Fui Theng Yap ©

A thesis submitted to the Faculty of Graduate Studies and Research in partial fulfillment of the requirements for the degree of Master of Science

Department of Chemical and Materials Engineering

Edmonton, Alberta

Fall 1996

National Library of Canada
Acquisitions and Bibliographic Services Branch
395 Wellington Street
Ottawa, Ontario
K1A 0N4

Bibliothèque nationale du Canada
Direction des acquisitions et des services bibliographiques
395, rue Wellington
Ottawa (Ontario)
K1A 0N4

Your file Votre référence

Our file Notre référence

ISBN 0-612-18338-6

University of Alberta

Library Release Form

Name of Author: Fui Theng Yap

Title of Thesis: One-step Oxidation of Ethylene to Acetic Acid using Hydrophobic Catalysts

Degree: Master of Science

Year this Degree Granted: 1996

323 Hawkview Manor Circle NW
Calgary, Alberta
T3G 2Y9
Canada

September 30, 1996

University of Alberta

Faculty of Graduate Studies and Research

The undersigned certify that they have read, and recommend to the Faculty of Graduate Studies and Research for acceptance, a thesis entitled One-step Oxidation of Ethylene to Acetic Acid using Hydrophobic Catalysts in partial fulfillment of the requirements for the degree of Master of Science.

KTChuang

Dr. K.T. Chuang

RGCavell

Dr. R.G. Cavell

SEWanke

Dr. S.E. Wanke

W. McCaffrey

Dr. W. McCaffrey

Date: Sept. 24, 1996

To my beloved parents,

Kim Yin and Sow Chan

Abstract

The demand for acetic acid has increased steadily over the years because of its use in the manufacture of paints, coatings and plastics. Industrial routes used in the commercial production of acetic acid are methanol carbonylation, acetaldehyde process and liquid phase oxidation of n-butane. Many research efforts are made directed toward the development of a better acetic acid process.

The main objective of this investigation was to study a catalytic process for the direct oxidation of ethylene to acetic acid in a slurry reactor containing a hydrophobic catalyst and water. Ethylene and pure oxygen were fed continuously into the reactor and the product from the reaction, acetic acid, was collected in the aqueous phase of the slurry reactor. The acetic acid yield achieved by these hydrophobic catalysts was approximately twenty times higher than those of the hydrophilic catalysts. The effect of important reaction parameters such as impeller speed, temperature, and pressure were experimentally determined. As temperature was increased, ethylene conversion improved but the selectivity deteriorated. High pressure was found to improve the catalyst activity. A by-product, carbon dioxide, was produced through the complete oxidation of ethylene. Several additives to the catalyst were examined for possible improvement in selectivity. Kinetic models based on proposed mechanisms of the reaction were used to fit the experimental data. The apparent activation energy for the formation of acetic acid was determined to be 23.72 kJ/mol.

Acknowledgments

I am grateful to Dr. Karl T. Chuang for his time and effort guiding me in this research with his technical expertise.

I also want to extend my warmest thanks to Dr. Bing Zhou for sharing his technical knowledge in catalysis and his advice concerning the operation of the equipment. Special thanks also goes to Dr. Shimin Tong for his guidance on data analysis in the later stage of my work. I would like to especially thank and acknowledge the help and advice from my colleagues: Mingqian Zhang, Dave Spagnolo, Gelai Kang, and Dr. Stefan Slavov.

A special note of thanks is due to the Department of Chemical Engineering and the Natural Sciences and Engineering Research Council of Canada for the financial support.

I want to express my sincerest gratitude to my parents for their unfailing love and support in every aspect of my life. I am especially thankful to my husband, Brian, for his patience and encouragement throughout my involvement in the research.

Above all, I want to thank God for his love and provision in guiding me through this stage of my life.

Contents

List of Tables

List of Figures

Chapter 1

Introduction

Acetic acid (CH_3COOH) is a corrosive organic acid having a pungent odor, burning taste, and pernicious blistering properties. It is found in ocean water, oilfield brines, rain, and at trace concentrations in many plant and animal liquids. Vinegar, produced by fermentation of wine, is a 4-12% acetic acid solution.

Acetic acid has a place in organic processes comparable to sulfuric acid in chemical industries. The major producers of synthetic acetic acid are the United States, Western Europe, Japan, Canada, and Mexico. The total production in these countries was close to 4×10^6 tons per year in the 1980s (Kirk and Othmer, 1992). Growth of synthetic acetic acid production in the United States was greatly affected by the dislocations in fuel resources of the 1970s. Since then, the demand for acetic acid has increased steadily over the years. The growth rate for 1988 was 1.5% (Kirk and Othmer, 1992). Acetic acid is consumed mainly in the manufacture of vinyl acetate and acetic anhydride. Vinyl acetate is utilized in the production of latex emulsion resins used in paints, adhesives, paper coatings, and textile treatments. Acetic anhydride is used to manufacture cellulose acetate textile fibers, cigarette filter tow, and cellulosic plastics (Aguilo *et al.*, 1985).

There are a few commercial routes used in the manufacture of synthetic acetic acid. They are carbonylation of methanol, liquid-phase catalytic oxidation of saturated hydrocarbons, and acetaldehyde oxidation. Commercial production of acetic acid was revolutionized through the decade 1978-1988. Butane/naphtha liquid-phase oxidation has declined precipitously as methanol carbonylation has become the technology of choice in the world market. About half of the world production comes from methanol carbonylation. However, due to the use of expensive rhodium catalysts and severe operating conditions which result in high costs on equipment and safety measures, many research efforts are underway by the industry in order to develop a more cost-efficient process for acetic acid production.

A three-phase slurry reactor was selected as the reactor system for this study. In recent years considerable attention has been given to the use of slurry reactors for a variety of applications. Slurry reactors offer a number of advantages over fixed-bed reactors in terms of easy adaptability to continuous operation, maintenance of isothermal conditions, and longer life of catalysts (Misic and Smith, 1971; Komiyama and Smith, 1975). Even though metals such as cobalt, nickel, rhodium, and palladium are widely used in homogeneous system at commercial scale, there are potential advantages in supporting these catalysts on carriers. By doing so the catalyst can be easily separated from the reaction mixture and can possibly be used in continuous processes. Furthermore, some of these heterogenized catalysts can be easily regenerated and reused.

The main objective of this study was to examine the use of supported palladium catalysts in one-step oxidation of ethylene to acetic acid. Palladium plays an important role in olefinic oxidation. It had long been recognized as the catalyst in the oxidation of olefinic hydrocarbons to give vinylic products like acetaldehyde, acetone, and vinyl acetate (Lyons, 1988). But it has been reported that under mild conditions, olefins can also give allylic products over supported palladium catalysts suspended in water (Lyons, 1988; Sood, 1995).

In this study, palladium was supported on hydrophobic carriers made of polymeric materials. The reason for using hydrophobic supports is that low reaction rates are observed for a catalytic reaction that takes place in the aqueous phase when a hydrophilic support is used. The advantages of hydrophobic supports in reactions involving an aqueous phase has been recognized (Chauvin *et al.*, 1977; Lieto *et al*, 1983; Fu and Chuang, 1989; Kawakami *et al.*, 1988). The hydrophobicity of these supports reduces the mass transfer resistance by prohibiting the water molecules from wetting the pores of the catalyst. The hydrophobic property of their matrix may also protect the organometallic active center from catalyst deactivation caused by capillary condensation and slow water desorption (Chuang et al., 1994).

The selection of a suitable catalyst and the effect of several experimental parameters are examined in this thesis. Product yield and selectivity were used as a basis for the catalyst screening process. Preparation and characterization of the catalyst are presented. The

Brunauer-Emmett-Teller (BET) surface area for each support were measured by nitrogen adsorption and crystallite sizes and metal dispersions of palladium were determined from X-ray diffraction peaks. A kinetic model is also presented and it is fit to the kinetic data obtained experimentally. Even though the investigation of the mechanism was not the intent of this study, a mechanism is proposed for the kinetic model.

Chapter 2

Literature Review

Presented in this chapter are brief reviews of the commercial routes used to manufacture acetic acid and also those laboratory-scale processes being studied at the research and development level. A survey on the work that has been done and is related to the present field of research will also be discussed.

2.1 Industrial Processes for Acetic Acid

Commercial production of synthetic acetic acid started in the early 19th century. Presently, there are three industrial processes for the production of acetic acid. They are methanol carbonylation, liquid oxidation of saturated hydrocarbons, and acetaldehyde oxidation (Aguilo *et al.*, 1985). Oxidation of acetaldehyde, developed in the 1920s, is the oldest process among the three. Acetaldehyde oxidation is extensively employed in Europe where acetaldehyde is produced from the palladium-copper-catalyzed oxidation of ethylene. The process based on the oxidation of cheap liquid hydrocarbons was developed in the 1950s. Methanol carbonylation, a more selective route, was introduced by BASF ten years later. This high pressure process was later modified by Monsanto with the discovery of a new catalyst.

2.1.1 Methanol Carbonylation

Methanol and carbon monoxide are the raw materials for this process. It was first commercialized by BASF in 1960. It is a high-pressure (70 MPa), high-temperature (250°C) process in which homogeneous catalysts are used. The working catalyst is cobalt iodide. The capacity of this process has increased from 3600 tons/year initially to 45,000 tons/year in 1981(Aguilo *et al.*, 1985). Shown in Figure 2.1 is a typical flow diagram for methanol carbonylation.

The discovery of a new iodide-promoted rhodium catalyst with remarkable activity and selectivity was reported by Monsanto in 1968. The process was commercialized two years later and the plant expanded its capacity to 180,000 tons/year in 1975. Operating conditions are 3 MPa and 180 °C, which are milder than those for the BASF process. The reaction is exothermic and very selective, yielding only traces of propionic acid, a by-product (Lloyd D. I. *et al.*, 1993). Almost all new plants use this modified low pressure route. In the United States, the capacity of this process grew from almost nothing in 1969 to 80% of actual plant operational capacity in 1988.

Presently, methanol carbonylation is used to manufacture 60 percent of the acetic acid produced in the world. This technology is favored among the three commercial processes because of its high selectivity and low operating cost. However, exotic construction materials are required due to the corrosiveness of the system. Another minor drawback is that some CO is lost through a water-gas shift reaction (Kirk and Othmer, 1992).

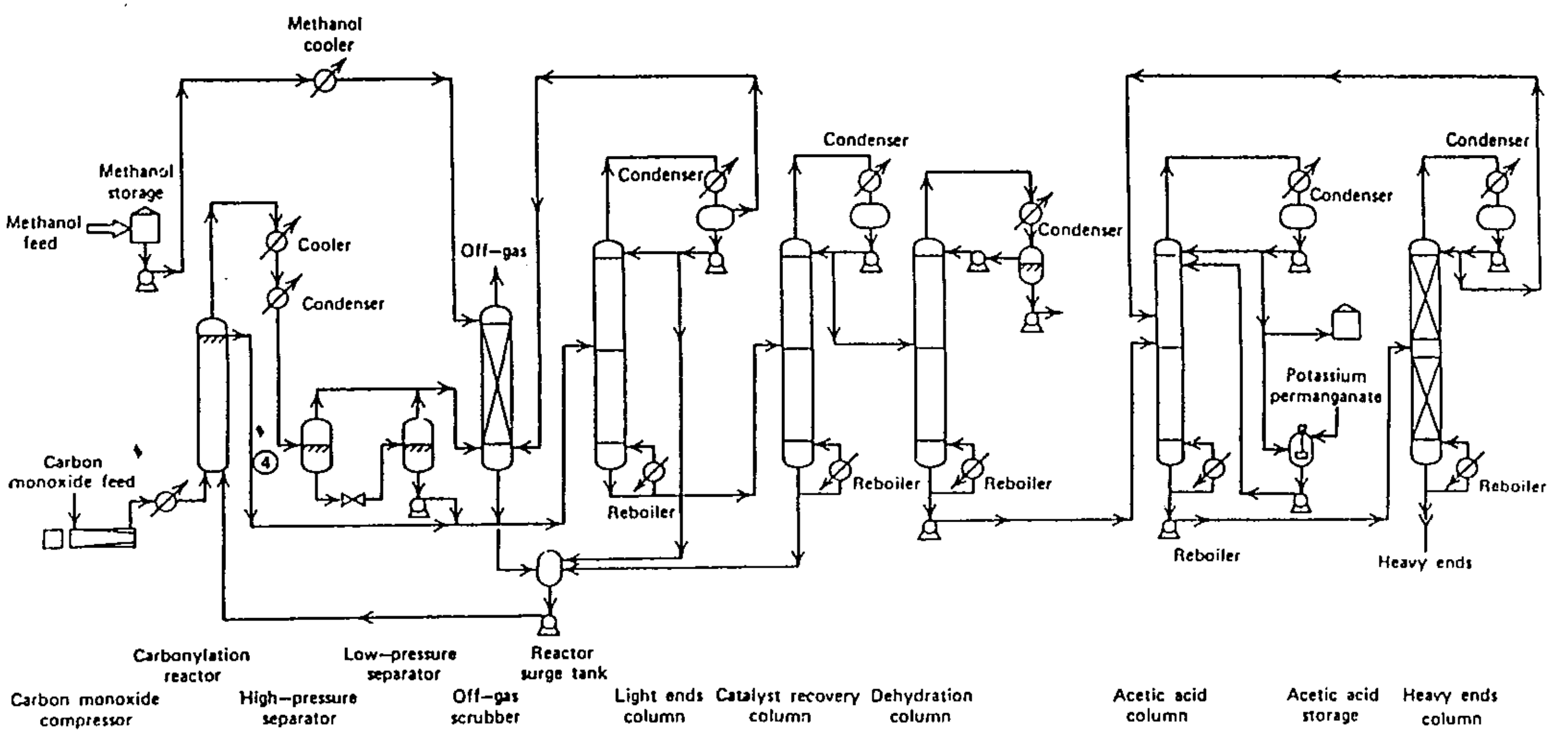

Figure 2.1 A typical methanol carbonylation flow diagram
(Kirk and Othmer, 1992)

2.1.2 Oxidation of Liquid Hydrocarbons

Aliphatic hydrocarbons such as n-butane and naphtha are suitable for the production of acetic acid. It was once the most favored world-wide route to produce acetic acid because of the low cost of the hydrocarbons. The process using n-butane has been operated on a large scale by companies such as Celanese and Union Carbide(Aguilo *et al.*, 1985). Figure 2.2 is a process flow sheet for n-butane oxidation. Butane, in the presence of metal ions such as Mn, Co, Ni, and Cr, undergoes simple oxidation in a sparged column. Operating temperature is kept just below the critical temperature of butane, 152°C. Pressure is about 5.6 MPa. The peroxidic intermediates are decomposed by high temperature, by mechanical agitation, and by action of the metallic catalysts, to form acetic acid and a comparatively small amount of other compounds.

The oxidation of naphtha is a noncatalytic operation. The operating conditions of this process are reported to be 150-200 °C and 5.6 MPa (Lloyd D. I. et. al., 1993). The reaction is propagated through free radicals and is highly exothermic and non-selective, yielding a wide range of oxidized gaseous and liquid products. The reactor outlet streams typically contain only 30 wt % acetic acid. As a result, a series of twenty columns are used to purify the products. The high recycling and purification costs make a newly-built plant unjustifiable. However, in addition to acetic acid, there are three co-products: formic acid, propionic acid, and acetone. The sale of these co-products actually reduce the variable costs of production. Therefore, a fully written down naphtha plant is still excellent in generating cash (Lloyd D. I. *et. al.*, 1993).

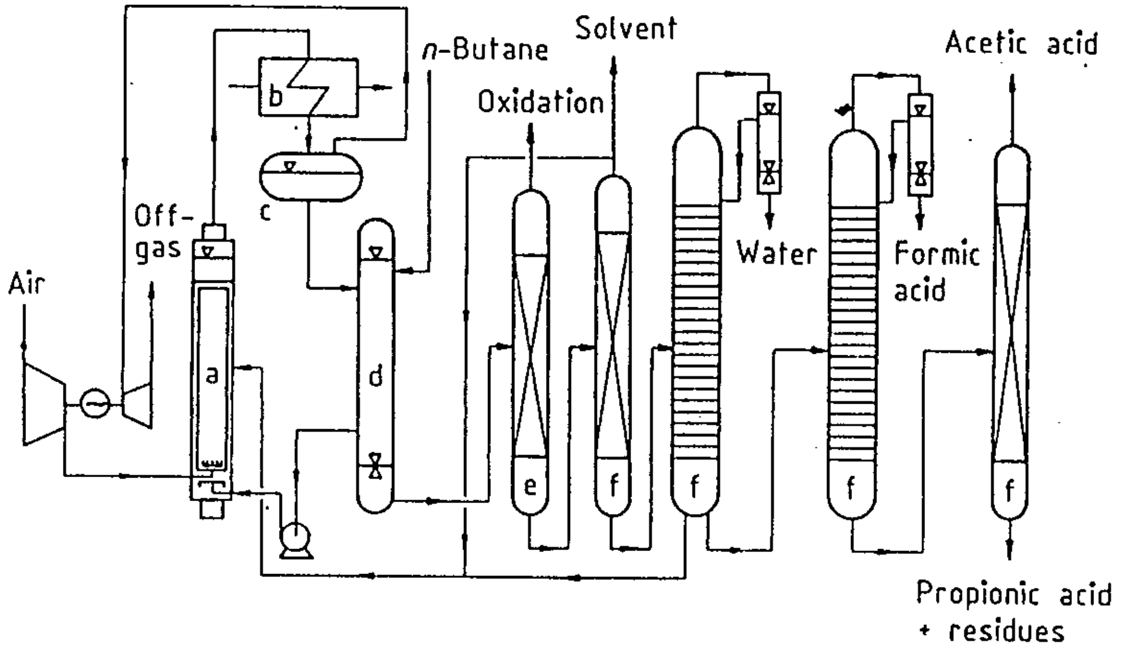

Figure 2.2 **Process flow diagram for the oxidation of n-butane** (Aguilo *et al.*, 1985)

a) Reactor; b) Air cooler; c) Collector; d) Separation vessel; e) Pressure column; f) Distillation column

2.1.3 Acetaldehyde Oxidation

This is an established process and widely used in Europe. Shown in Figure 2.3 is a process flow diagram for acetaldehyde oxidation. Acetaldehyde oxidation is a two-stage oxidation process: an initial step to form acetaldehyde either from ethylene or alcohols, which is then further oxidized to give acetic acid. Presently, more than 80% of acetaldehyde used in the production of acetic acid is formed by direct oxidation of ethylene (Kirk and Othmer, 1992).

The first stage where ethylene is oxidized to acetaldehyde, also known as the Wacker-Hoechst process, uses aqueous solutions of $PdCl_2$ and $CuCl_2$ as the homogeneous catalysts. Different catalysts, either cobalt or manganese salts, are used for the second stage where the oxidation of acetaldehyde to acetic acid takes place. The operating conditions of the reactor are at temperatures of 60-80 °C and pressures of 0.3-1.0 MPa (Aguilo *et al.*, 1985). Crude oxidate is passed to the recovery column where unreacted acetaldehyde is recycled. The reaction product is purified by an azeotropic distillation tower. Ethyl acetate is used in some operations to entrain water and formic acid in the finishing column.

Conversion of acetaldehyde is typically more than 90% and selectivity to acetic acid is higher than 95%. The problems that exist are related to more extensively automating control of the system, especially at start-up and shutdown. Because the catalysts used in the two stages differ from each other, direct synthesis of acetic acid by this process is

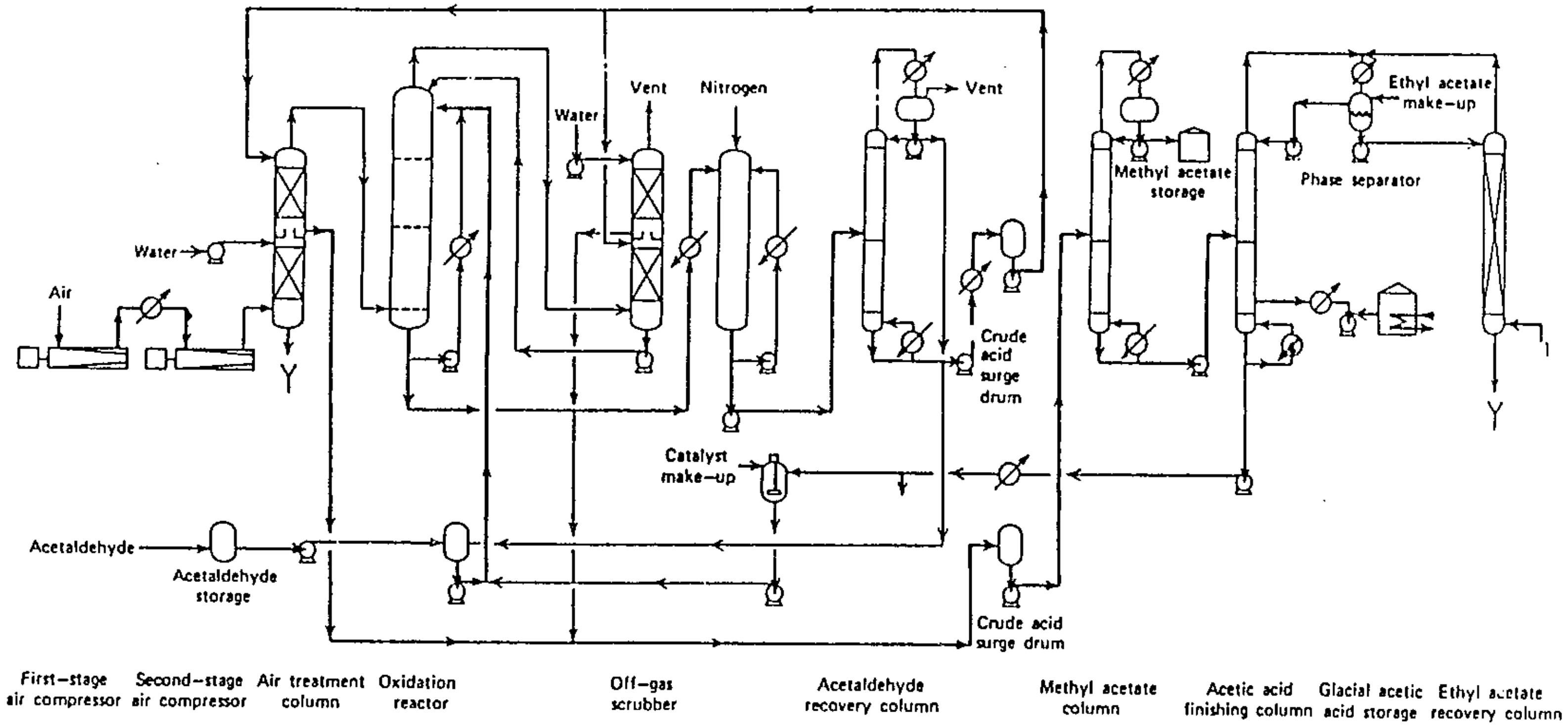

Figure 2.3 A typical acetaldehyde oxidation flow diagram (Kirk and Othmer, 1992)

difficult. Also, high capital and operating costs result from the complexity of the process. Therefore, even though the operating conditions are milder compared to the methanol carbonylation and liquid phase oxidation of hydrocarbons, it is no longer feasible to manufacture acetic acid through this process (Aguilo *et al.*, 1985).

2.2 Prospective Processes

There has been much research effort invested in developing a new acetic acid process. Routes that have been investigated are the Showa Denko process (vapor phase oxidation of ethylene), oxidation of n-butene in the vapor phase, and the oxidation of sec-butyl acetate (Aguilo *et al.*, 1985). The cost of the raw materials is generally prohibitive. So far, none of these processes has been commercialized. However, the Showa Denko process and the oxidation of butenes have been developed to pilot plant scale.

2.2.1 The Showa Denko Process

Ethylene is used as the raw material to form acetic acid in this one-step vapor phase oxidation process. A stable catalyst, comprising metallic palladium and at least one member selected from the group consisting of heteropoly-acids and their salts, which exhibits a high yield and low selectivity of carbon dioxide was discovered. The palladium was supported on silica in an amount of 0.01 to 6.0 % by weight (Suzuki *et al.*, 1994).

A fixed bed reactor system was adopted and an amount of 15 mL of catalysts were packed into a reaction tube. The feed gas is a mixture of ethylene, oxygen, steam and nitrogen. Operating temperatures were in the range of 140 to 200 °C and reaction pressure was approximately 1.4 MPa (200 psig). The exit gas was cooled, condensed and collected as a liquid to be analyzed by a gas chromatography (Suzuki *et al.*, 1994).

2.2.2 The Chemische Werke Huls Process

This process is the vapor-phase oxidation of n-butenes at 180-245°C and 200-3000 kPa over a titanium-vanadium oxide catalyst. The acetic acid yield for this process is 46%. The oxidation is carried out in the presence of air and steam in a fixed-bed tubular reactor. The heat of reaction is recovered through process steam generation. Purification is carried out in four towers: a high-ends column, a drying column, a formic acid separation column, and a finishing column (Aguilo *et al.*, 1985).

2.2.3 The Bayer Process

The n-butenes first react with acetic acid at 100-120 °C and 1.9 MPa, to produce sec-butyl acetate. The sec-butyl acetate is then catalytically oxidized in the liquid phase at 200 °C and 6.3 MPa. The overall process yield of acetic acid is 58%. Purification is by conventional method using four towers (Aguilo *et al.*, 1985).

2.3 Ethylene Oxidation over Metal Catalysts

Oxidation of ethylene leads to a variety of valuable oxygen containing products such as ethylene oxide, acetaldehyde, formaldehyde and acetic acid. Therefore, the choice of selective catalysts for the above reactions is of great practical importance. Silver catalysts are used in the synthesis of ethylene oxide via partial oxidation of ethylene. The complete oxidation of ethylene into carbon dioxide and water on platinum was observed during the early nineteenth century. Oxidation of ethylene on palladium was found to start at a temperature as low as 50 °C (Golodets, 1983). Acetic acid, together with carbon dioxide and water, was formed (Kemball and Patterson, 1962). Since then, the synthesis of acetic acid on palladium has been of special interest.

2.4 Role of Palladium in Olefinic Oxidation

Palladium is a unique element in many respects. It is in the Ni triad (Ni, Pd, Pt) of the Group 10 elements. It has a high melting point (1552 °C) and boiling point (2964 °C) and is very resistant to corrosion. Many of its uses are related to its corrosion resistance. Examples are dental alloys, jewelry and electrical contacts. The metal has a d^{10} electronic configuration. Chemically palladium has been used extensively as a heterogeneous catalyst. The catalytic chemistry of palladium metal results from the ability of its active center to coordinate unsaturated organic ligands. Once in the coordination sphere, the metal is able to induce transformations which eventually result in a catalytic reaction.

Palladium compounds are also convenient reagents since they are usually stable and easy to handle. Toxicity is not a serious concern. However, palladium is an expensive metal. The current cost of palladium is US $125/oz (Colonial Metals, Inc., 1996).

Palladium has been used extensively in olefinic oxidation and hydrogenation reactions. It represents one of the most industrially important classes of oxidation catalysts especially after the ingenious Wacker-Hoedst process was developed in 1959. In the Wacker-Hoedst process, palladium (II) salt, is used as a homogeneous catalyst to convert ethylene into acetaldehyde. This process, developed by Smidt and coworkers, actually consists of three separate reactions (Henry, 1980):

$$PdCl_4^{2-} + C_2H_4 + H_2O \rightarrow CH_3CHO + Pd(0) + 2HCl + 2Cl^-$$

$$Pd(0) + 2CuCl_2 + 2Cl^- \rightarrow PdCl_4^{2-} + 2CuCl$$

$$2CuCl + \tfrac{1}{2}O_2 + 2HCl \rightarrow 2CuCl_2 + H_2O$$

That is: (i) the oxidation of ethylene to acetaldehyde by palladium (II) in aqueous solution, (ii) the conversion of palladium(0) to palladium(II) by cupric chloride *in situ*, and (iii) the regeneration of cupric chloride from cuprous chloride using air in aqueous solution. In addition to the Wacker-Hoedst type oxidation of olefins, many reactions involving palladium compounds have been discovered in the last 20 years. These reactions, consisted of a series of related catalytic reactions, are responsible for the manufacture of other oxidation products such as acetone and vinyl acetate. These reactions occur either in solutions of palladium complexes or over heterogeneous supported palladium catalysts.

Patterson and Kemball (1963) first reported that small amounts of acetone together with carbon dioxide were produced in the catalytic oxidation of olefins over palladium film. Later it was also found that propylene can be oxidized to acrylic acid and acrolein at high selectivity in the presence of palladium black suspended in water (Seiyama *et al.*, 1972). The synthesis of acrylic acid from propylene can also be achieved over supported palladium catalysts under mild conditions in the presence of water (David *et al.*, 1971; Lyons *et al.*, 1988; Sood, 1995).

Kemball and Patterson (1962) reported the formation of acetic acid via the oxidation of ethylene over palladium. Since then, palladium has been proposed in many studies to be the potential catalyst for commercial production of acetic acid. For example, supported palladium with heteropoly-acids as catalyst modifying agents is examined and found effective in the Showa Denko process. Palladium metal with phosphoric acid as the modifying agent is also examined in an acetic acid process by a Japanese company (Suzuki *et al.*, 1994).

2.5 Chemistry of Olefinic Oxidation on Palladium

Many recent studies have been done on the chemistry of olefinic oxidation, especially for heterogeneous reactions involved the use of palladium. For oxidation of olefins with three carbon atoms or higher, the comparison between vinylic and allylic routes has been the topic of interest. Lyons (1988) argued that the catalytic oxidation of propylene and butene using palladium produces vinylic products via direct nucleophilic attack on palladium-olefin π-complexes. Carbon-hydrogen bond cleavage (β-hydrogen elimination) takes place after nucleophilic attack has occurred. These reactions can be made to occur catalytically in the presence of palladium either in homogeneous solution or over heterogeneous supported catalysts.

In the catalytic oxidation of olefins over metallic palladium suspended in water, it was found that the formation of a π-allylic complex from olefin is the initial step in the oxidation on the palladium metal surface (Seiyama, 1972). This takes place if C-H activation can be encouraged to occur before nucleophilic attack rather than after; and allylic products, such as acrylic acid, allyl acetate. and methacrylic acid, rather than vinylic oxidation products will result (Lyons, 1988). Lyons (1988) also reported that the formation of the π-allylic complex can be achieved not only on surface, but also in solution species of palladium (Eq 2.1, 2.2).

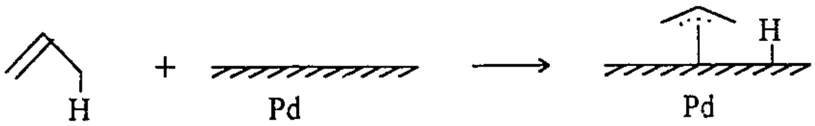

(2.1)

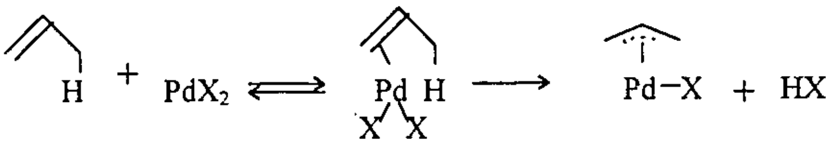

(2.2)

Factors which affect the route in olefinic oxidation were considered. It was suggested that in the presence of a poorly coordinating weak base, predominant allylic oxidation occurs

(Swodenk and Scharfe, 1975; Stolyarov et al., 1982). The function of the base is to remove a proton to form a palladium π-allyl complex as the catalytic intermediate (Chrisope and Beak, 1986). The nature of the ligand system about the palladium(II) complex also can determine whether vinylic or allylic oxidation predominates. It has been suggested that Pd(II) complexes with strongly electron withdrawing ligands are highly electrophilic and oxidatively add an allylic C-H bond to form π-allyl intermediates directly (Trost and Metzner, 1980). In the case of heterogeneous palladium catalyst, a high oxidation state will promote vinylic oxidation. Addition of strong oxidant or the presence of halide ions which can increase the oxidation state of palladium will also promote the formation of vinylic oxidation products (Lyons, 1988).

Chapter 3

Catalyst Preparation and Characterization

This chapter outlines the preparation and characterization of the catalysts used in this study. They were characterized in terms of their BET surface area, particle size, and metal dispersion. The basis for the selection of catalyst supports and active components for the reaction will also be presented.

3.1 Selection of the Catalyst Support

Supported catalysts are one of the conventional catalysts used in the chemical industry. The first step in this study was to select an optimum support material under the criteria of surface area, inertness, thermal stability, mechanical strength, and cost. The hydrophobicity of the support is considered as an important factor for this particular three phase reaction. It has been shown that a catalyst supported on hydrophilic material such as alumina, silica, and silica-alumina, loses its activity due to capillary condensation of water and slow water desorption (Sherwood, 1981; Chuang *et al.*, 1994). Although some of these supports exhibit high selectivity, reaction rates are generally several orders of magnitude lower than those reported for the vapor phase reaction. The reason for low activity can be explained using the Kelvin equation (Golodets, 1983):

$$\ln(P/P_o) = -2\,V\,\tau\,\cos\theta/(rRT) \tag{3.1}$$

where R = gas constant

r = radius of the capillary

V= molar volume of the liquid

τ = surface tension

θ = contact angle

Equation (3.1) suggests that for a contact angle less than 90°, liquid condenses in the capillary at a pressure P less than the saturation pressure P_o at a temperature T. The contact angle of hydrophilic supports with an aqueous solution is close to zero. Therefore, all of the surfaces of the catalyst are wet when exposed to liquid. For a mass transfer limiting reaction, it is difficult for reactants such as ethylene and oxygen with low solubility and low liquid-phase diffusion coefficients to reach the surface of the catalyst. Hence, low activity is resulted due to mass transfer resistance.

The contact angle of hydrophobic supports with water is higher than 90°. Therefore, the pore will remain dry and accessible to the reactant gasses as the chances of the pores being wetted is greatly reduced. As a result, mass transfer resistance is decreased dramatically. The advantages of polymeric supports over conventional supports have been recognized widely (Chauvin *et al.*, 1977; Leito *et al.*, 1983). They are considered to be catalytically inert, easily functionalized, and can be prepared with a wide range of physical properties.

Their relative poor thermal stability is the only drawback but it is not a concern in this study as the operating temperature is relatively low.

Polystyrene-divinylbenzene (SDB), a high purity polymeric catalyst support, is a copolymer of styrene and divinylbenzene:

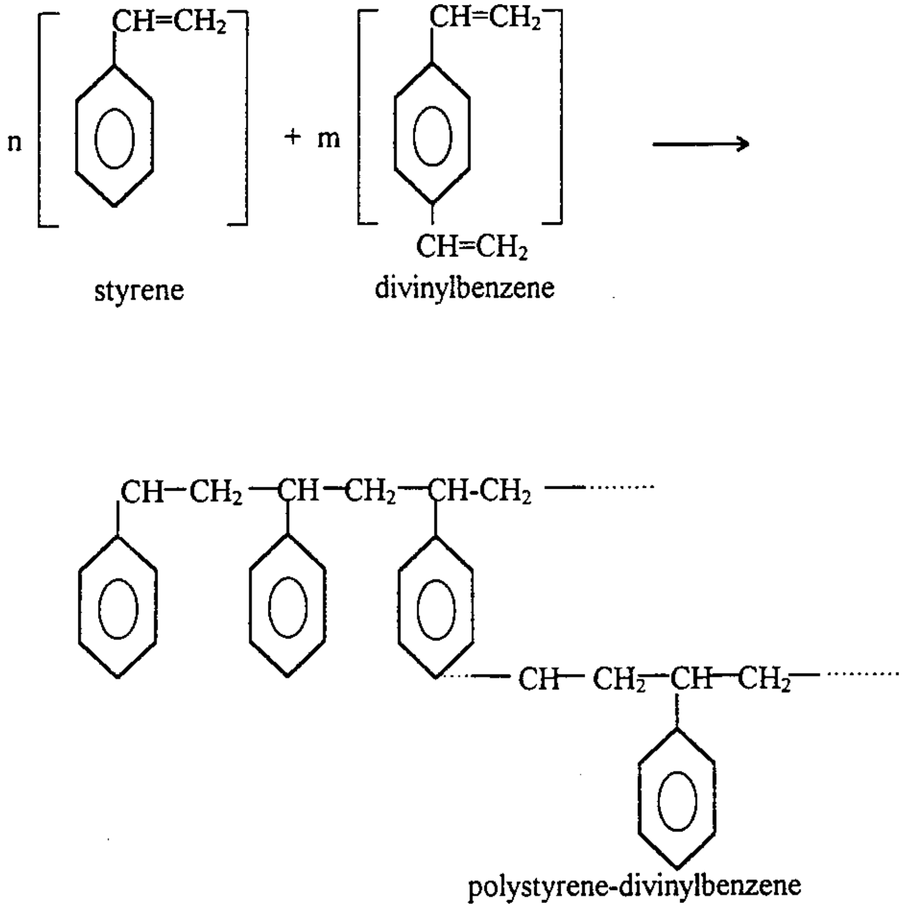

Figure 3.1 Molecular structure of polystyrene-divinylbenzene

The SDBs are reported to be effective in the partial oxidation of olefins such as propylene (Sood, 1995). It is also reported to be used extensively in a number of reactions such as, the reduction of NO_x with H_2 (Fu and Chuang, 1989), CO oxidation in humid air (Yaparpalvi and Chuang, 1991), and the removal of hydrogen and oxygen from explosive mixtures (Ledjef, 1987). Furthermore, their properties and characteristics meet most of the criteria of an industrial catalyst support. These hydrophobic supports are inert, mechanically stable, and very porous. These supports remain thermally stable up to 250°C.

For this study, SDBs were obtained from Hayes Separation Incorporated and Porapak Incorporated. Alumina is included in the study to show the advantage of hydrophobic supports. Alumina powder is obtained by grinding 1/8" γ-alumina spheres from La Roche. Their characteristics are listed in Table 3.1. Values of the BET surface area are obtained from the manufacturers.

Table 3.1 Physical characteristics of various supports

Support	BET Surface area (m^2/g)	Mesh Size
HayeSep D	795	> 50
Porapak Q/QS	634	80-100
γ-alumina	235	>100

HayeSep D has the highest BET surface area but its mesh size is slightly lower than other supports. On the other hand, BET surface area for the γ-alumina is three times lower than that of HayeSep D.

3.2 Selection of Metal Loadings

Noble metals belonging to group 10 have been reported to be effective in liquid phase oxidation of olefins (Seiyama *et al.*, 1972; Chuang and Fu, 1993). These metals were recognized for their excellent capacity for chemisorbing gases such as ethylene and oxygen (Le Page, 1987). Furthermore, mature catalysis technology in our laboratory involving these metals has been successfully applied to benzene-toluene-xylene (BTX) oxidation, formaldehyde oxidation, and synthesis of acrylic acid. Therefore, palladium, platinum and nickel are examined in this study for their suitability in converting ethylene to acetic acid. The activities of these metal catalysts in olefin oxidation are Pd > Pt > Ni in decreasing order (Seiyama et al., 1972; Le Page, 1987). Metallic palladium was found to be effective in converting ethylene to acetic acid in a vapor process (Suzuki, 1994). In fact, since the development of the Wacker process, catalytic reactions of olefins using palladium salts have been studied by many researchers (Stern, 1968). As a result, palladium was chosen as the main catalyst for this research. Platinum and nickel were added in small amount in addition to palladium to determine their effects on the reaction. Different combination of metal loadings were investigated for their activity and selectivity. Table 3.2 summarizes these combinations with the metal loadings supported on different supports.

Table 3.2 Various combination of metal loading

Catalyst Support	Metal Loading
HayeSep D	10% Pd, 9% Pd + 1% Pt, 10% Pd + 1% Ni
Porapak Q	3% Pd, 10% Pd, 3% Pd + 0.045% Pt
Porapak QS	10% Pd
γ-alumina	10% Pd

3.3 Preparation of Catalysts

The method of catalyst preparation can change with the choice of base material. Even for a given selection of base material, experience shows that several ways of preparing the catalyst can be considered. Table 3.3 lists the various unit operations involved in catalyst preparation (Le Page, 1987).

Table 3.3 Unit operations of catalyst preparation

1. Precipitation	7. Forming operation
2. Hydrothermal transformation	8. Calcination
3. Decantation, filtration, centrifugation	9. Impregnation
4. Washing	10. Mixing
5. Drying	11. Activation
6. Crushing and grinding	12. Special operation

Preparation of a given catalyst will require putting these operations into a characteristic order. Although preparation processes vary considerably from one catalyst to another, the processes by which the majority of the industrial catalysts are manufactured can be grouped into three broad categories according to their products (Le Page, 1987), as:

(1) Bulk catalysts and supports.

(2) Impregnated catalysts on preformed supports.

(3) Mixed-agglomerated catalysts.

As mentioned earlier, the catalysts used in this study belong to the second type: impregnated catalyst on preformed supports. The following preparation procedure for the catalyst is similar to that reported in previous studies (Sood 1995). The unit operations in sequence are impregnation, drying, and a special operation: reduction.

3.3.1 Pd/SDB

The following method is applicable to any SDB supports that are used in this study. The Pd/SDB catalysts were prepared by impregnation of SDB with the methanolic solution of the precursor salt, $PdCl_2$ (supplied by Colonial Metals, Inc., U.S.A.) and followed by reduction using hydrogen gas. The precursor salt solution was prepared by completely dissolving $PdCl_2$ into a 20% hydrochloric acid solution. The amount of the precursor salt required was calculated on the basis of intended metal loading. The impregnation of the SDB was achieved by first soaking the weighed supports with methanol followed by the addition of the dissolved $PdCl_2$ to facilitate wetting of the pores by the effect of the capillary forces. The operation was relatively rapid. The mixture was then immediately mounted onto an atmospheric rotary evaporator under infra-red light and left to dry overnight, or at least for a period of 12 hours. The drying process facilitated the precursor to crystallize onto the pores of the supports. Rapid drying was important as it favored a finer deposit of crystals (Le Page, 1987). The dried mixture was then packed into a glass U-tube and placed into a furnace for reduction. The reduction temperature was set at 250°C and controlled by an Omega programmable temperature controller. Reduction was achieved by continuously supplying hydrogen gas at 100 mL/min for 12 hours. Nitrogen was used before and after reduction for flushing. The reduced catalyst was allowed to cool to room temperature before it was ready to be used.

3.3.2 Pd-Pt/SDB, Pd-Ni/SDB

A slightly modified impregnation procedure was used for a catalyst with the combination of palladium, platinum and nickel as the active components. For impregnation of platinum, the $(NH_3)_4Pt(NO_3)_2$ solution provided by Johnson Matthey Co. was used. A 4% platinum solution, prepared from $(NH_3)_4Pt(NO_3)_2$, was added once the $PdCl_2$ was completely dissolved in the hydrochloric solution. On the other hand, the $Ni(NO_3)_2$ powder from BDH was added to the precursor solution for the impregnation of nickel. For the catalysts with combination of noble metals, only the impregnation step was modified. The remaining steps, namely the drying and reduction steps, remained unchanged.

3.4 Characterization of Catalysts

Heterogeneous catalysis is a surface phenomenon. It is not enough just to have the required elementary composition formed during preparation. There must also be the largest possible active surface for any given mass of catalytic material and this active surface must be topographically arranged so as to facilitate the access of reactants and the departure of products. Therefore, it is important to examine the physico-chemical characteristics of the catalytic solid. In order to characterize each catalyst, X-ray diffraction was used.

3.4.1 BET Surface Area

Nitrogen adsorption was performed on the supports using Omnisorp 360. The BET surface area for the different supports was measured. Comparison between the measured and the manufacturers' values is summarized in Table 3.4. The measured values of the BET area for each support are very close to those quoted by the manufacturers.

Table 3.4 BET surface area of various supports

Support	BET surface area (m^2/g)	
	Measured	Manufacturer
HayeSep D	736	795
Porapak Q/QS	634	634
γ-alumina	237	235

3.4.2 Crystallite Sizes and Metal Dispersion

Supported catalyst particles are usually found to have very simple shapes: spheres or hemispheres are most common whereas cubes and plates are less frequently observed. Therefore, only spherical particles will be considered in what follows. The characteristic size will be simply the diameter of the spheres. Particle sizes for some catalysts were determined from the measurements made by X-ray diffraction. X-ray line broadening analysis (XLBA) is applied to estimate the size of small crystallites. Figure 3.2(a) is a X-ray diffraction spectra for 10% palladium supported on HayeSep D. Scherrer's formula relates average crystallite size to the breadth of the peak at half intensity as follows (Cullity, 1967):

$$t = \frac{0.9\,\lambda}{\beta_{1/2}\cos\theta} \tag{3.2}$$

where

t = crystallite size

λ = X-ray wavelength

$\beta_{1/2}$ = breadth of the peak at half intensity

The breadth of the peak at half intensity, $\beta_{1/2}$, can be measured from the X-ray spectra as shown in Figure 3.2(a). The Bragg angle of diffraction, θ, can be directly obtained from the Powder Diffraction File (JCPDS, 1989).

Presented in Figures 3.2(a) to 3.2(d) are the X-ray diffraction spectra for 10 % palladium supported on carriers that were examined. As observed, the peaks for palladium crystallite supported on the polymeric carriers are broader compared with that for γ-alumina which has the narrowest peak indicating the largest crystallite.

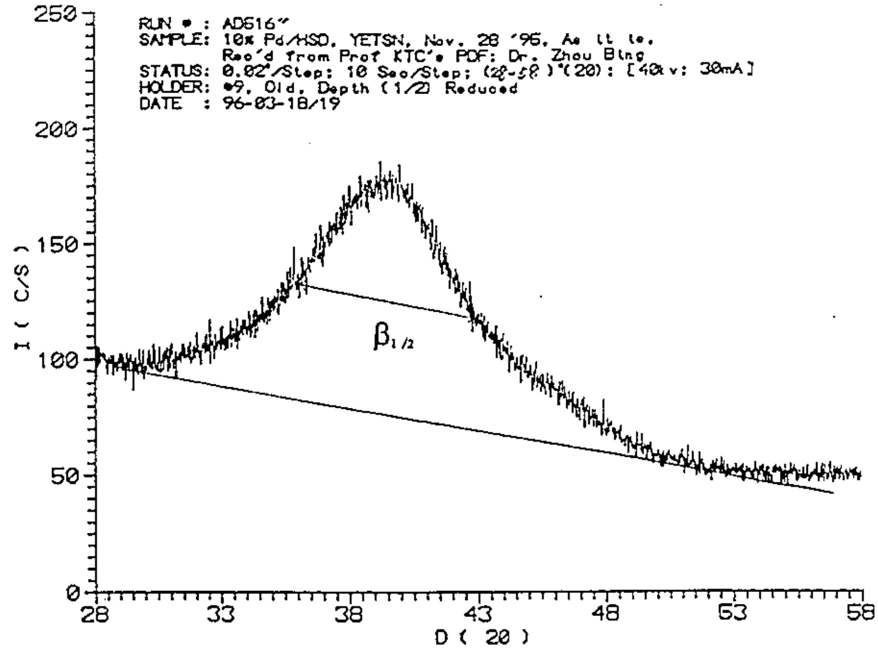

3.2(a) X-ray diffraction pattern for 10% Pd/HayeSep D

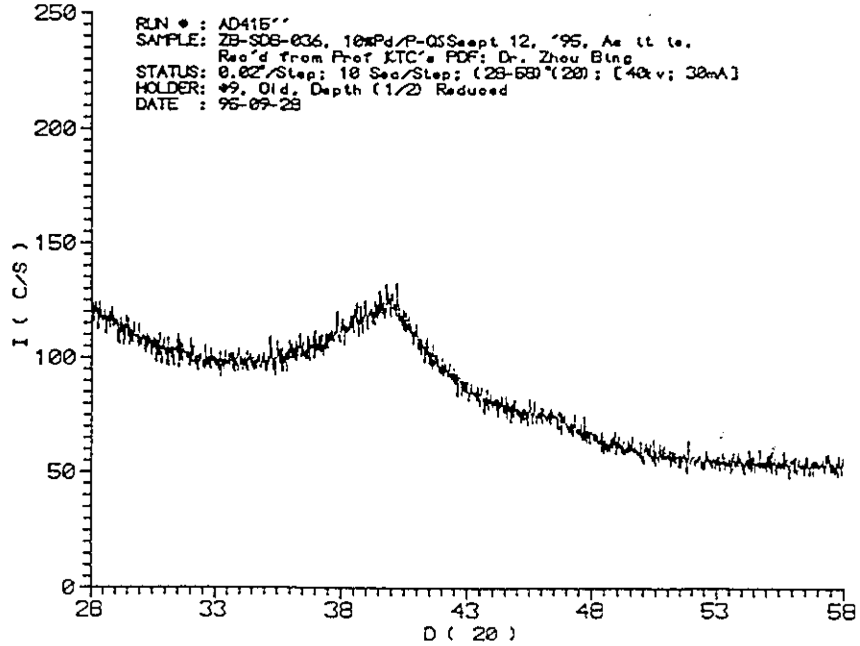

3.2(b) X-ray diffraction pattern for 10% Pd/Porapak QS

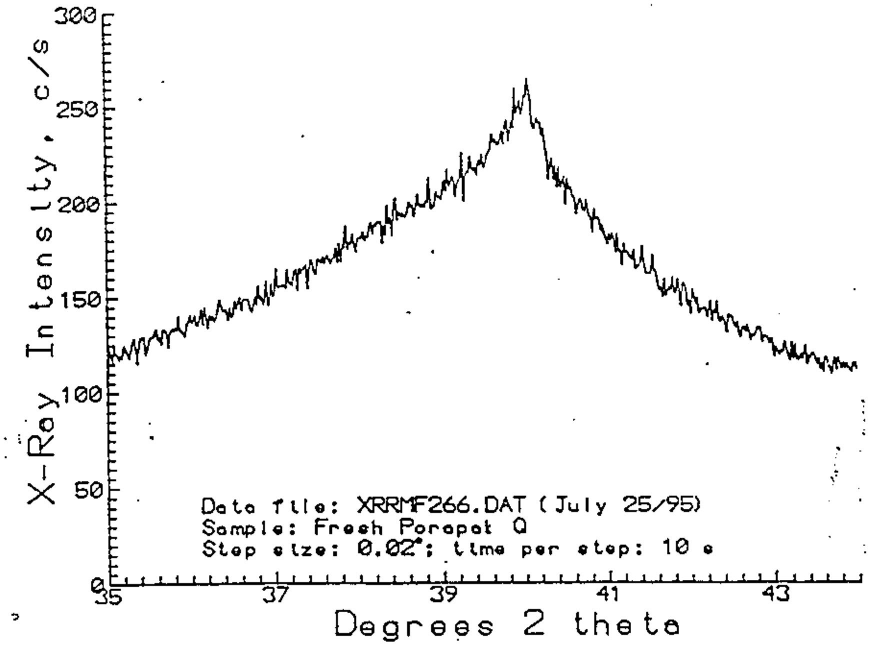

3.2(c) X-ray diffraction pattern for 10% Pd/Porapak Q

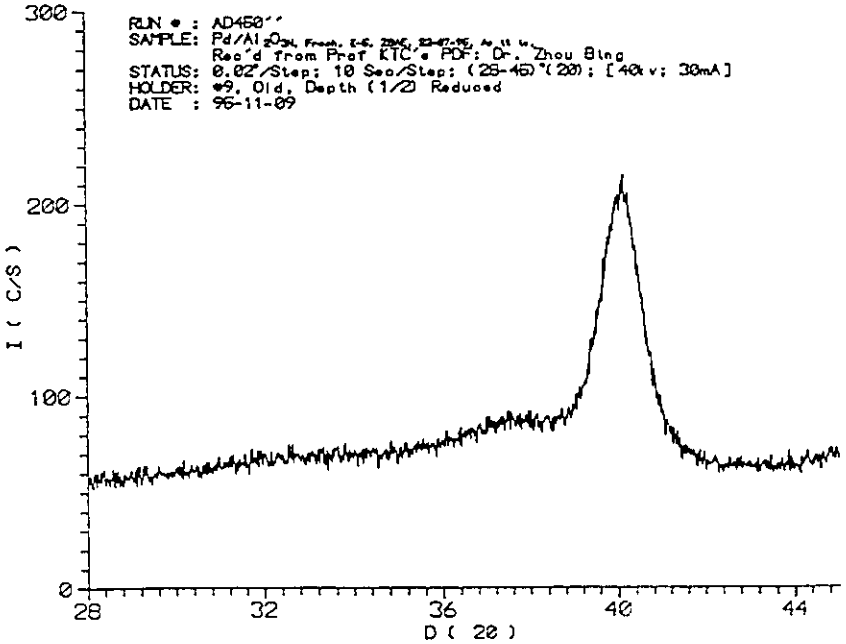

3.2(d) X-ray diffraction pattern for 10% Pd/γ-alumina

The activity of heterogeneous catalysts is known to be influenced by their surface properties. In the case of supported catalysts containing expensive active substances such as noble metals, it is important to reduce the amount of active component without affecting the overall activity by increasing the surface-to-volume ratio. This ratio of the active component is usually referred to as dispersion. Therefore, optimum dispersion is of particular economic importance for catalysts having noble metals as the active components.

There are several ways to determine metal dispersion. Chemisorption, X-ray diffraction, transmission electron microscopy and XPS peak intensity measurements are the several schemes used to estimate metal dispersion of catalysts (Delannay, 1984). The X-ray diffraction was the technique used in this study to characterize the heterogeneous catalysts. From the X-ray diffraction data, palladium dispersion for each catalyst can be calculated using the estimated crystallite sizes obtained from XLBA.

Metal dispersion is defined as the ratio of the number of active atoms exposed at the surface, N_s, to the total number of active atoms present in the catalyst, N_t (Anderson and Pratt, 1985):

$$D = \frac{N_s}{N_t} \tag{3.3}$$

and Ns and Nt can be defined as

$$N_s = \frac{A_p}{A_a} \tag{3.4}$$

$$N_t = \frac{V_p}{V_a} \tag{3.5}$$

where A_p = Area of particle surface = πd_p^2

Aa = Atomic area = $\frac{A_{100} + A_{110} + A_{111}}{3}$

A_{100} = 100 face atomic area

A_{110} = 110 face atomic area

A_{111} = 111 face atomic area

Vp = Volume of particle = $\pi d_p^3/6$

and Va = Atomic volume = $\frac{M_a}{N_o} \times \frac{1}{\rho_{Pd}}$

Therefore, dispersion can now be related to the particle size d_p, atomic weight M_a, density ρ_{Pd}, atomic area A_a and Avogadro's number N_o by the following equation:

$$D = \frac{6}{d_p} \times \frac{M_a}{\rho_{Pd} A_a N_o} \tag{3.6}$$

Atomic weight, density, and atomic area of palladium are 106.4 g/mol, 12.0 g/cm^3, and 9.496 Å^2 respectively. If the crystallite size, t, obtained from X-ray diffraction, is assumed to be equal to the particle size d_p, then palladium dispersion can be expressed as follows:

$$D = \frac{6\,M_a}{t\,\rho_{Pd} A_a N_o} \tag{3.7}$$

The crystallite sizes and the metal dispersion of palladium for each catalyst is estimated and summarized in Table 3.5.

Table 3.5 Crystallite sizes and palladium dispersion for various catalysts

Catalyst	Crystallite Size (nm)	Metal Dispersion (%)
10% Pd/HayeSep D	1.29	72.07
10% Pd/Porapak Q	3.39	27.42
10% Pd/Porapak QS	2.56	36.23
10% Pd/γ-Alumina	7.69	12.08

As shown in Table 3.5, γ-alumina, which is a hydrophilic support, has a particle size of two to six times larger and a dispersion of two to six times lower than those of hydrophobic supports. The relatively low dispersion for palladium supported γ-alumina is due to the low BET surface area of γ-alumina. As shown in Table 3.4, γ-alumina has a BET surface area of 3 to 3.5 times lower than that of the SDBs. On the other hand, HayeSep D, which has the highest BET suface area, has the smallest palladium particle size and highest dispersion among the hydrophobic supports examined in this study.

Chapter 4

Experimental Setup and Procedure

This chapter contains the details of the experimental setup and procedure used in this study. The experimental equipment and apparatus are similar to those of a previous study reported by Sood (1995). Analytical techniques used to determine the product assays are also included in this chapter.

4.1 Experimental Setup

A schematic diagram of the entire flow reactor system is shown in Figure 4.1.

4.1.1 The Reactor

The oxidation of ethylene was carried out in a stirred tank reactor supplied by Parr Instrument Co. The 300-mL reactor had an internal diameter of 6.32 cm and was made of 316 stainless steel. A four-bladed disc turbine impeller 20 mm in diameter was used for agitation. The speed of the impeller was adjusted by a variable speed motor and the shaft was connected to a magnetic drive. Inlet and outlet lines to the reactor were connected to 6.35-mm ID high strength Teflon tubing.

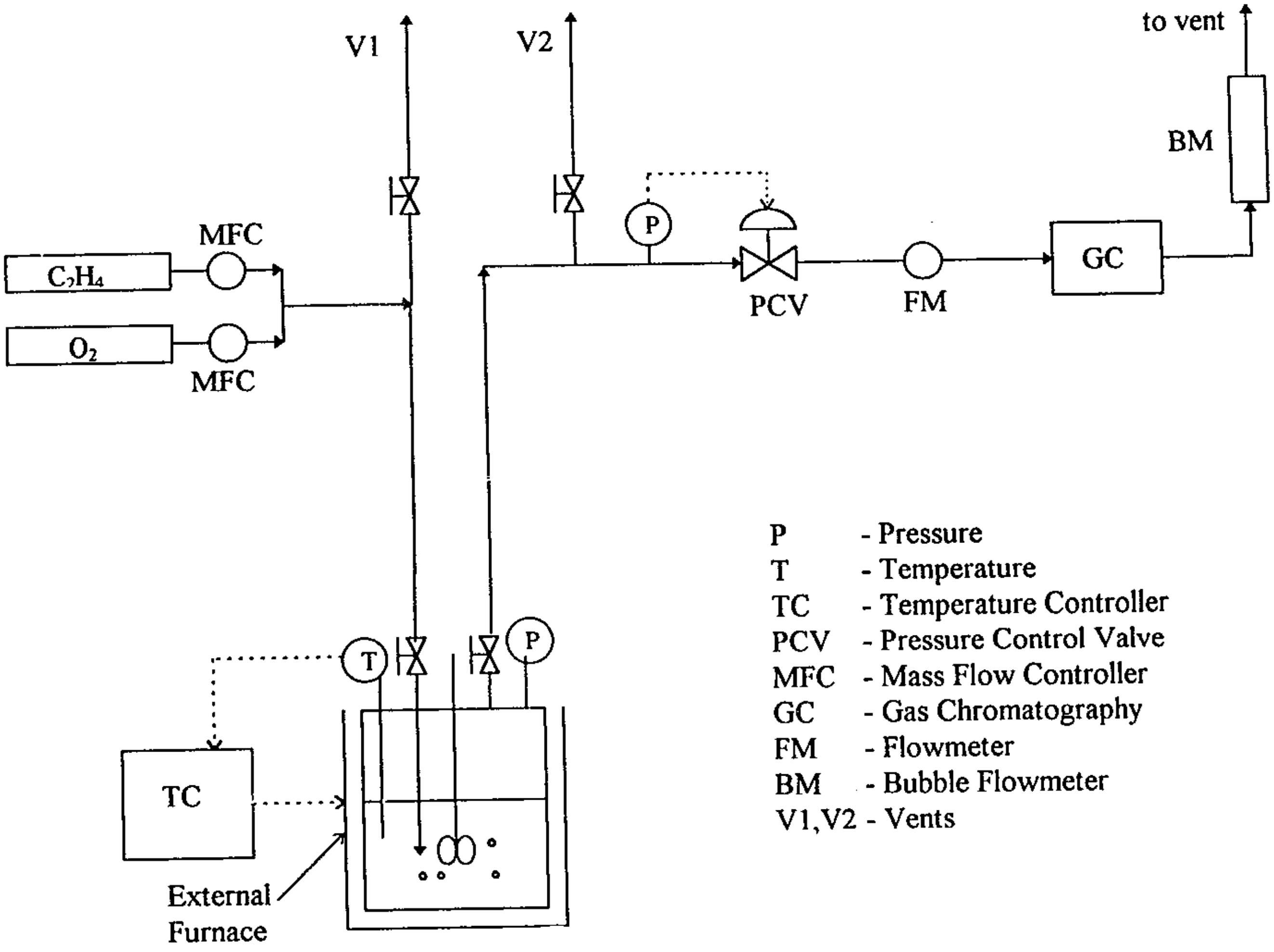

Figure 4.1 Schematic diagram of the flow reactor system

4.1.2 The Gas Flow System

The feed gas to the reactor contained high purity ethylene and oxygen. Pure oxygen was used because air has about 80% diluent. For industrial application, it is not practical to use air as it is necessary to remove the diluent or nitrogen from the exit gas before ethylene is recycled into the system. The feed gas, ethylene and oxygen, were supplied from standard gas cylinders; ethylene and extra-dry oxygen gas cylinders were provided by Matheson Gas and Praxair Canada Inc. respectively. After pressure reduction with two-stage regulators, the two gases were passed through mass flow controllers. Flow rates were monitored by Unit and Brooks mass flow controllers and flow-meters. Total volumetric flow rates of feed gased were maintained at 50 mL/min for all of the tests. The gases were mixed at a tee fitting before they were introduced into the system through a small tube. Fluctuation of flow occurred only occasionally and normal values were established in the order of seconds. The exit stream leaving the reactor flowed through a pressure control valve for controlling the pressure in the reactor and then through the sample loop of a gas-sampling valve in a gas chromatograph before the total exit gas flow rate was measured and vented.

The total pressure of the system was regulated by a feedback control system. The controlling mechanism started with a pressure sensor reading the reactor pressure and sent the information to a Shimaden PID controller. This information was compared with the set point value and sent a signal to the control valve to monitor the percent opening of the pneumatic valve attached downstream of the reactor exit line. This feedback control system maintained the total pressure within ±1 psi of the set value.

The temperature during the reaction was monitored by a similar feedback control system with a Parr 4841 external heater which was connected to a thermocouple immersed into the liquid of the reactor system. The thermocouple sent the signal to the temperature controller which regulated the temperature inside the reactor with an accuracy of ±1°C.

4.2 Explosion Limits of Ethylene

Attention to explosion limits is absolutely required for a process that involves potentially explosive gases such as ethylene. In recent years a number of chemical processes have been developed in which ethylene is partially oxidized to give a wide variety of products such as acetaldehyde and ethylene oxide. Most processes involve the mixing of ethylene with either air or oxygen and the contacting of these reactants with various catalysts. In order to ensure the safe operation of such chemical processes it is necessary to know the explosion limits of the reactants and the products involved under the prevailing conditions of temperature and pressure. In the industrial production of ethylene oxide, the reactions are carried out with oxygen and an excess of ethylene, above the upper explosion limit. Specified by the supplier, the upper explosion limit of ethylene is 73.0 volume % ethylene in pure oxygen. The lower explosion limit is 13.5 volume % ethylene in pure oxygen (Aguilo et al., 1985). For safety reasons and because of the low mass flows required for experiments in the slurry reactor, feed ratios above the upper explosion limit were chosen.

4.3 Analysis of Gas Samples

Outlet gas from the reactor was sent for periodic sampling to determine the exit gas composition. Using the gas-sampling valve, samples of exit gas at atmospheric pressure and room temperature were injected into a Hewlett-Packard Model 5170 gas chromatograph equipped with a thermal conductivity detector (TCD). A 2.4-m long stainless steel column packed with 80-100 mesh Porapak R was used for the analysis of ethylene, oxygen, and carbon dioxide. The detection limit is 50 ppm. Water was detected in the exit gas but in insignificant amount. No other possible by-products such as methanol, acetaldehyde, formaldehyde, ethylene oxide, and carbon monoxide were detected in the exit gas samples. The helium carrier gas flow rate was maintained at 20 mL/min at ambient conditions and the column oven was operating isothermally at 80 °C. Pure ethylene, pure oxygen, and 5 % carbon dioxide in nitrogen, supplied by Praxair, were used as the standard gases to calibrate for the gas chromatography.

4.4 Analysis of Liquid Samples

Determination of the amount of acetic acid produced for each experimental run was carried out using acid-base titration with sodium hydroxide. It was initially done using buret titration but was later switched to a Mettler DL21 titrator. Duplicate samples weighing 5 to 10 g from each sample were analyzed and an average was calculated. The parameters of the titrator could be customized to the particular liquid sample being analyzed. Connected to the titrator was an on-line printer. On one end of the titrator was a glass dispenser of NaOH while a stirrer and the sample container were fitted on the other end. Each titration run was initiated by pressing the run button on the key panel and pulses of 0.1g of titrant were injected into the sample to be titrated. The results of each run were printed after the system had reached its equivalence point. The titrator was highly reliable and the data were reproducible. Duplicate runs of the same sample gave deviations of less than 1% in the required volume of titrant.

To further confirm that the main product collected in the liquid sample was acetic acid, samples were injected into a HP 5890 Gas Chromatography with two detectors, namely the flame ionization detector (FID) and the thermal conductivity detector (TCD). The GC was equipped with a capillary column and a programmable oven. The oven temperature was set at 35 °C during the first two minutes and increased to 130°C at a rate of 15°C/min. Injected sample was analyzed with both detectors connected in series. Qualitative calibration was performed during the initial period of the research to ensure that the two significant peaks obtained were of acetic acid and water. Formic acid, which is a possible by-product collected in the liquid samples, was not detected. A very small peak of acetaldehyde was detected by FID. The peak was too small to trigger an integration. Thus, the amount was insignificant compared with the acetic acid concentration.

4.5 Experimental Procedure

A series of screening experimental runs were performed to examine the activity and the selectivity of catalysts. With the prior knowledge of the reactor feed gas flow rates and the outlet gas total flow rate and its composition, performance characteristics such as ethylene conversion, oxygen conversion and acetic acid selectivity could be determined. Upon identification of a potential catalyst, subsequent experiments were carried out to determine the effects of catalyst composition and reaction parameters such as temperature, pressure, impeller speed, and feed composition. Preliminary kinetics was studied by varying feed composition and obtaining the Arrhenius plot of the oxidation reaction of ethylene at different temperatures.

Feed gas flow rates were calibrated very frequently or when there was a change in feed compositions. A typical calibration procedure started with at least an hour of stream line flushing with the feed gas, which was ethylene in this case. Flow rate was measured with a bubble flowmeter and a stop watch and was adjusted by changing the set point of the mass flow controller. Flow rate measurements were taken when flow rates were stable indicated by a steady reading of the mass flow meter. After a desired flow was obtained for ethylene, the line was purged and charged with oxygen. The calibration of oxygen was difficult compared to that of ethylene because low oxygen flow rate (5-12 mL/min) was required for most of the test runs. In fact, results of some test runs were discarded because of the unacceptable flow rate discrepancy from the set point value. After the desired flow rates for both feed gases were achieved, they were allowed to mix for at least two hours to assure a steady state composition was reached. Finally the calibrated feed gases was sampled using the on-line GC to confirm the feed ratio.

In a typical run, 1.00 g of catalyst and 100 mL of deionized water was initially put into the reactor. Because of the hydrophobicity of the catalyst, it initially floated on the surface of the water. In order to observe the flow pattern upon stirring, a glass reactor with similar dimensions was used. It was observed that the system behaved like a slurry reactor. The catalyst was distributed uniformly upon stirring. Feed gases were allowed to purge the reactor for approximate 10-15 minutes before start-up by closing the ball valve to vent V1 and opening the reactor inlet and outlet needle valves. Even though different feed compositions were used, the total volumetric flow rate of feed gas remained at 50 mL/min. To start up, the valve to the bypass line of the pressure control valve would be closed for the system pressure to build up to the set point value. When the pressure reached 60 psig, the heater and the stirrer were switched on. It took approximately 80 min for the system pressure to reach 120 psig. For test runs at 200 psig, the start up time could take up to 2h. Measurements were made every hour starting the first hour after the pressure and temperature had reached the operating values. This consisted of measuring the total exit flow rates and taking GC samples of the reactor exit gas. Approximately 8-10 readings were taken for the total exit flow rates using the bubble flow meter and a stop watch. Two samples were usually routed to the GC column to determine the volume percents of ethylene, oxygen and CO_2 that were in the exit gas. The duration of each test run was 5-6 hours. To shut down the experiment, the heater and stirrer were turned off, followed immediately by shutting off the reactor inlet and outlet valves. The valves to vent V1 and V2 were then opened to release the pressure within lines upstream and downstream of the reactor. The valves of gas cylinders were then closed. The reactor was cooled to room temperature by immersing into an ice-water bath. The pressure inside the reactor was then released by opening the outlet valve slowly. The reactor was dissembled and a large portion of the liquid sample was collected by gravity filtration for analysis. The used catalyst was washed several times with water and dried overnight for catalyst characterization or reuse.

4.6 Blank Run

A blank run without catalyst was carried out at 120 psig and 110 °C. No acetic acid was detected in the liquid product. Hence, it can be concluded that catalysts are required for the partial oxidation of ethylene to acetic acid. Throughout the course of the experiment, one percent of ethylene was converted and approximately 400 ppm of carbon dioxide was detected in the exit gas through samplings of gas chromatography. Since an operating temperature of 110 °C is too low for thermal reaction to take place, it therefore may suggest that the reactor wall, the impeller, and related parts that came into contact with the liquid acted as catalysts for the deep oxidation of ethylene. The 316-stainless-steel reactor was made from 60% Fe and approximately 40% other metals such as Cr, Ni, and Mo. These metals were reported to be excellent catalysts for deep oxidation of trichloroethylene for the study of VOC destruction (Greene *et al.*, 1995). Deep oxidation started at temperatures as low as 100°C and total conversion was achieved at 350°C.

In order to ensure that these metals were not affecting the reaction especially for those kinetic runs, the impeller and related parts that came into contact with the liquid during experiment were coated with Teflon and a glass liner was fitted into the reactor.

4.7 Material Balance

Material balance was performed for each test run. Mole balance on carbon is carried out as follows:

$$\text{In} - \text{Out} + \text{Generation} = 0 \qquad (4.1)$$

where

In = 2 x Ethylene inlet flow rate in mol/h x Experimental length in hours

Out = 2 x Σ (Hourly measurement of ethylene outlet flow rate in mol/h)

+ Σ (Hourly measurement of carbon dioxide outlet flow rate in mol/h)

$$\text{Generation} = 2 \times \frac{\text{total acetic acid produced in grams}}{60.05}$$

A relative error of the molar balance can be measured using the following equation:

$$\text{Relative error of molar balance} = \frac{\text{In} - (\text{Out} + \text{Generation})}{\text{In}} \times 100\% \qquad (4.2)$$

Mole balance for the test runs revealed that the experimental error had been minimized to a relatively low value. Almost ninety percent of the test runs had a relative error of less than 5% on the carbon molar balance.

4.8 Definitions of Catalyst Performance Parameters

$$\text{Ethylene conversion} = \frac{\text{ethylene in} - \text{ethylene out}}{\text{ethylene in}} \tag{4.3}$$

$$CO_2\ \text{selectivity} = \frac{CO_2\ \text{produced}}{2 \text{ x ethylene reacted}} \text{ x } 100 \tag{4.4}$$

$$\text{Selectivity} = 100 - CO_2\ \text{selectivity} \tag{4.5}$$

$$\text{Yield} = \frac{\text{grams of acetic acid produced}}{\text{gram Pd x hour}} \tag{4.6}$$

Chapter 5

Results and Discussion

The results of this study are presented in the following section along with a discussion of observations made during the experimental tests. A series of tests to identify a suitable catalyst support and metal loading were carried out in order to optimize the acetic acid yield and selectivity. The effect of operating parameters such as pressure, temperature, feed ratio, impellers speed were also examined. An attempt to estimate the activation energy of the reaction provides a preliminary study on the reaction kinetics.

5.1 Catalyst Screening

The objective of the screening process was to determine which catalyst has the best performance in converting ethylene to acetic acid in the presence of pure oxygen. Screening of catalyst supports was performed before various metal loading combinations were tested on the selected support.

5.1.1 Screening of Catalyst Supports

In this study, γ-alumina, which is hydrophilic and widely used as a catalyst support, along with several hydrophobic supports were examined for their performance to demonstrate the advantages of hydrophobic supports in the reaction. In order to screen the catalyst supports, test runs at the same experimental conditions were performed. The total feed gas was controlled at 50 mL/min with 75% ethylene, the pressure set at 120 psig, the temperature set at 90°C and an allowed reaction time of 6 hours. All the supports were loaded with the same amount of palladium metal. Results are summarized in Table 5.1. The yield in grams of acetic acid per gram of palladium per hour was used as the basis for comparison. Selectivity was also included as a secondary guideline to screen each catalyst.

Table 5.1 Performances of various supports loaded with 10% Pd

Support	Yield (g CH_3COOH/gPd-h)	Selectivity (%)
HayeSep D	1.56	88.5
Porapak Q	1.42	86.7
Porapak QS	1.38	89.1
γ-alumina	0.08	99.1

The product yield for the four supports have shown that the performance of hydrophobic supports are almost twenty times better than that of γ-alumina. This is attributed to the hydrophobicity of the supports which decrease the mass transfer effect by keeping the water molecules away from the catalyst surface. The high selectivity of γ-alumina is probably due to the effect of surface concentrations of the reactants since internal diffusion is often a problem observed when hydrophilic catalysts are suspended in aqueous solution. It is also observed that HayeSep D has the best performance among the three hydrophobic supports and hence was selected to be the catalyst support for further detailed studies. The results also revealed that all three hydrophobic supports have similar selectivity.

5.1.2 Selection of Metal Compositions

Different combinations of metal composition were impregnated on HayeSep D and Porapak Q at the screening stage. Palladium was chosen as it has been proven a suitable catalyst for the gas phase conversion of ethylene to acetic acid (Suzuki et al., 1994). Other metals such as platinum and nickel were added in small amounts along with palladium in an attempt to improve the conversion of ethylene and the selectivity. The operating conditions for these tests were at 120 psig and 110 °C and the duration was six hours for each test. A temperature of 110 °C was used so that the effect of each metal on the catalyst performance would be more apparent. The feed composition was kept at 75% ethylene and HayeSep D was the support. The results of these experiments are presented in Table 5.2.

Table 5.2 Effects of platinum and nickel on catalyst activity

Catalyst	Yield (g CH_3COOH/g Pd-h)	Acetic Acid Selectivity (%)
10%Pd/HS-D	4.22	80.8
10%Pd+1%Ni/HS-D	2.20	81.3
9%Pd+1%Pt/HS-D	3.50	72.9

As observed from Table 5.2, addition of trace nickel caused a significant degradation in the activity of the catalyst and as a result, the yield was almost half of when palladium was the active component alone. It was also found that the presence of nickel has no influence on the selectivity of catalyst. However, ethylene oxidation tends to go to complete oxidation in the presence of a small amount of platinum and resulted in a decrease in selectivity. Therefore, it is fair to conclude that palladium by itself is most effective in the conversion of ethylene to acetic acid.

5.1.3 Selection of Metal Loadings

In order to determine the effect of metal loading on the catalyst activity, a lower metal loading (3 % palladium) was examined. These tests were run at 120 psig and 90 °C with feed composition fixed at 75% ethylene and Porapak Q used as a support. These tests were performed before an optimum support was selected, therefore, Porapak Q was used since it was successfully applied in several processes that were examined by our catalysis laboratory. These test results are summarized in Table 5.3.

Table 5.3 Effect of metal loading on catalyst activity

Metal Loading	Yield (g acetic acid/g Pd-h)	Ethylene Conversion (%)	Acetic Acid Selectivity (%)
3% Pd	1.24	3.78	85.8
10% Pd	1.42	5.56	86.7

As seen from Table 5.3, the yield of acetic acid produced by the catalysts loaded with 3 % palladium is 20% less than that of catalyst with 10% palladium. The higher yield for the 10% loading catalyst is due to its better ethylene conversion, which is 5.56 %. The test results also show that the selectivity for the two different loadings are comparable, less than 1% difference.

Table 5.4 compares the particle size of palladium crystallites and its metal dispersion between 3% and 10% palladium loading. The catalyst with 3% loading has the smallest particle size, which is 1.06 nm, and the highest dispersion if compared with all other catalysts tested in this study (see Table 3.5).

Table 5.4 Comparison between 3% and 10% loading

Palladium Loading	Crystallite Size (nm)	Dispersion (%)
3 %	1.06	87.86
10 %	3.39	27.42

Particle size, which relates to metal loadings, is important and worth looking into as particle size effect was reported to remarkably improve the activity of $Ag/\alpha\text{-}Al_2O_3$ in ethylene epoxidation (Goncharova *et al.*, 1995). Goncharova *et al.* (1995) also showed that the particle size effect resulted from the change of the metallic surface; and the change of active surface structure affects adsorption of ethylene and oxygen, and thus, the reaction rate. Theoretically, catalysts with higher dispersion would have a better activity. However, the results shown in this study suggest the contrary. This may suggest that the oxidation of ethylene is a stucture sensitive reaction.

5.2 Comparison with the Showa Denko Process

Research and development efforts on new acetic acid processes have been significant. As mentioned in Chapter 2, there are several routes being investigated. The Showa Denko process, which is also a one-stage oxidation process of producing acetic acid from ethylene, uses similar catalysts to those investigated in this study. In addition to metallic palladium, a heteropoly-acid and its salts are supported on a hydrophilic carrier. The supports used in the Showa Denko process are silica and titania. The gas phase reaction was taken place in a plug flow reactor. The following table presents the product yield and selectivity of the Showa Denko process (Suzuki *et al.*, 1994) and of the present study.

Table 5.5 Comparison with the Showa Denko process

Process	Feed Ratio C_2H_4:O_2	Operating Conditions	Yield (g HAc/g Pd-h)	Selectivity (%)
This Study				
Pd/HayeSep D	7:1	120 psig, 130 °C	3.36	73.6
Showa Denko				
Pd/Silica	7:1	71 psig, 150 °C	1.86	78.5
Pd-Se/Silica	8:1	114 psig, 160 °C	4.80	86.4

As observed from Table 5.5, the catalyst investigated in this study is almost 50% more effective than the one examined by Showa Denko process when palladium was used alone as the active component. Therefore, supports play an important role in the activity of a catalyst. The product yield and selectivity of the palladium-selenium combination of the Japanese study (Suzuki et al., 1994) is higher compared with that of the catalyst used in this study. However, the three phase process in this study has an advantage over the Showa Denko process as temperature control is not a concern since the reactor system is close to isothermal. The mixing of the slurry reactor is so good that even for highly exothermic or endothermic reactions, the temperature is nearly the same in all parts of the reactor. The relatively high thermal conductivity of liquids increases the heat transfer coefficient. When this is coupled with the small heat of reaction per unit volume of the slurry, there is little temperature difference between the particle and the liquid. Thus, external temperature differences can normally be neglected in slurry reactors. For the Japanese process, run-away reactions are not the only problem. Corrosion is another major consideration since the vapor phase reaction is operating at relatively high temperature. As a result, more sophisticated construction materials and higher maintenance costs are anticipated.

Another main difference between the two processes is the means of product purification. For the Showa Denko process, an absorption unit will be suitable to separate acetic acid from the exit gas stream. On the other hand, a highly energy-intensive unit, namely a distillation unit, is required in product purification for the process proposed in this study. In order to compete with the low capital cost of the Japanese process, which is estimated to be only half of the capital cost of today's commercial processes, energy cost for the three-phase process must be lowered. This can be achieved if a concentrated acetic acid solution, say 50 %, is used as the starting solution. Another possible alternative for acetic acid purification is solvent extraction, especially for dilute acetic acid solutions. This type of solvent has been developed by companies such as Dow Chemicals (Aguilo et al., 1985).

5.3 Effect of Impeller Speed

In the process of examining the effect of stirring speed, different rpms were tested. Figure 5.1 summarizes the effect of these impeller speed on catalyst activity. Curve fitting of the data points showed that there is a maximum for the ethylene conversion curve. Duplicate runs were carried out to confirm this behavior.

It is observed that selectivity decreases with an increase of impeller speed. As seen from Figure 5.1, conversion improved but acetic acid selectivity dropped as the impeller speed increased from 300 to 500 rpm. However, as the impeller speed continued to increase, both ethylene conversion and acetic acid selectivity dropped. This is a rather interesting behavior. In order to understand the behavior, a glass reactor of similar dimensions as the stainless steel autoclave was used to examine the flow pattern of the stirred mixture.

As stir speed increases from 300 to 500 rpm, mass transfer resistance was expected to be reduced due to better mixing. Indeed, it was observed that the catalyst was distributed uniformly in the working solution. The unusual behavior in conversion and selectivity occurred when the impeller speed was above 750 rpm can be explained from the flow pattern observed as presented in Figure 5.2.

A vortex with almost half the depth of the working solution was formed around the impeller due to vigorous stirring. Because the density of the catalyst (approximately $0.35 g/cm^3$) is lower than the density of water, most of the catalyst was gathered near the

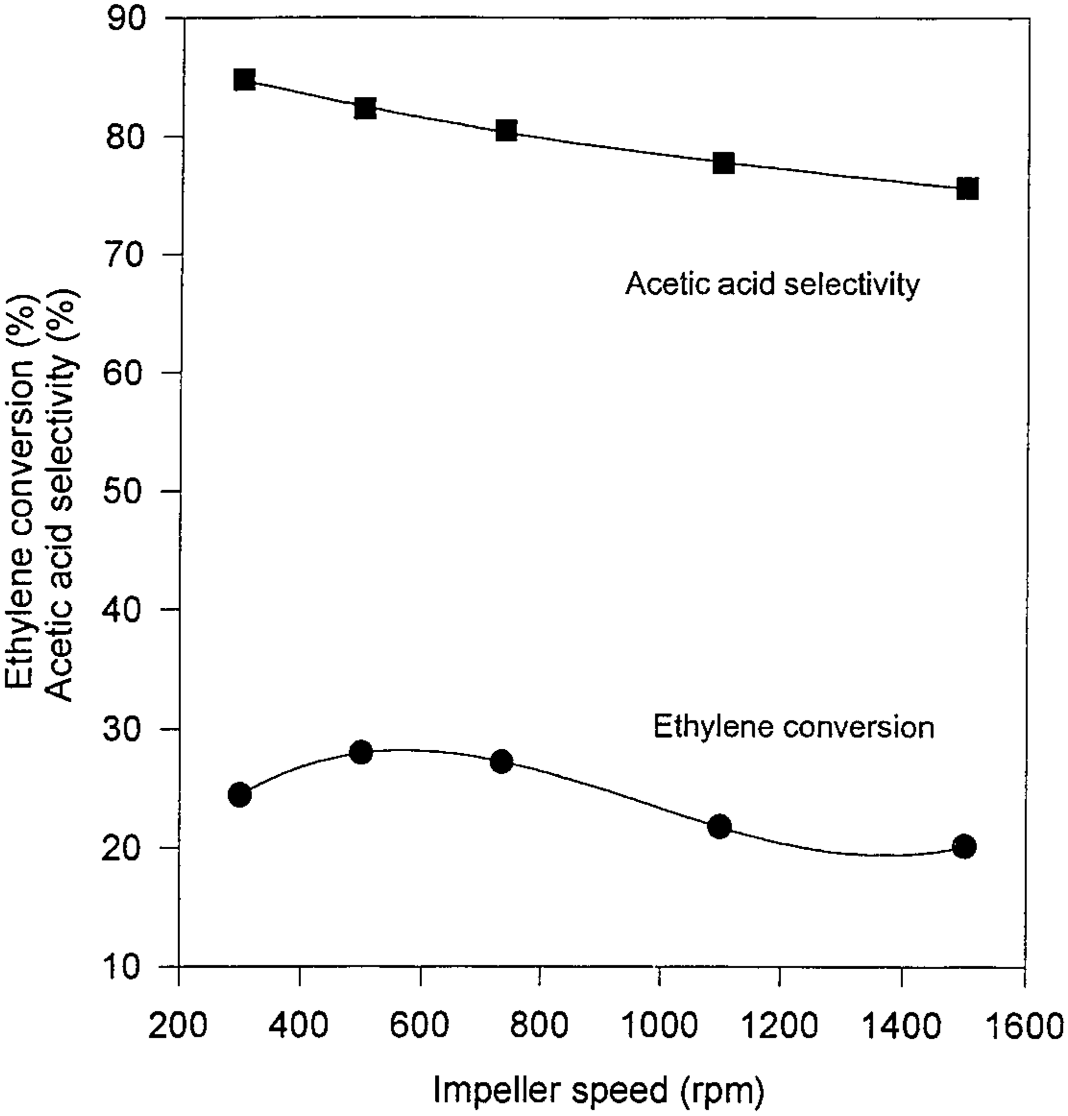

Figure 5.1 Effect of impeller speed on catalyst activity

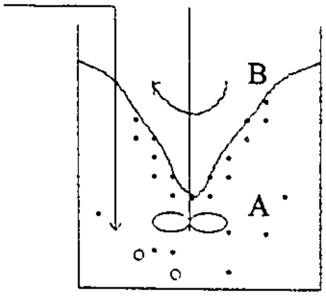

Figure 5.2 Flow pattern at impeller speed > 750 rpm

vortex and the working solution was thrown to the reactor wall. As a result, the conversion dropped as the catalysts were not uniformly distributed in the working solution. Most of the inlet gas bubbles bypass the catalyst in the solution. Also, as the stirring speed increased, more catalyst would be concentrated near the vortex. Shown in Figure 5.2, A and B are the two sections of the reactor system. Section A has the same gas composition as the feed gas. The vapor phase, section B, has the exit gas composition which is a lot richer in ethylene. Because these catalysts at the vortex were bypassed by most of the gas bubbles in section A as the stirring speed increased, they were exposed to the gas in section B more readily. Figure 5.1 shows that the reaction was less selective in forming acetic acid as the impeller speed increased, so it may suggest that the formation of carbon dioxide was more desirable when the catalyst were exposed to the gas that was richer in ethylene. This assumption may be supported by the results found in Section 5.7 where the effect of feed composition on catalyst activity was examined.

5.4 Effect of Temperature

Experimental runs were conducted at different temperatures to determine the effect of operating temperature on conversion and selectivity. These test runs were carried out with 10% palladium supported on HayeSep D, with 90% ethylene feed composition, and at a pressure of 120 psig. The operating temperatures were 90° to 130 °C.

The relationship between ethylene conversion and acetic acid selectivity with the five temperatures is shown in Figure 5.3. Because oxygen was the limiting reactant, ethylene conversion was relatively low. It can be seen that the conversion increases with the increase in temperature. This type of relationship was expected because gas molecules collided with each other more as temperature was increased. Figure 5.3 also presents how selectivity varies with temperature. The acetic acid selectivity on the other hand decreases with the increase in temperature. This behavior was also observed in the study of propylene oxidation on a similar catalyst by Sood (1995). An explanation for the decrease in acetic acid selectivity is that a higher activation energy is required for the complete oxidation to take place. Hence, formation of carbon dioxide tends to improve at a higher operating temperature.

As the test results show, an increase in temperature improves ethylene conversion but on the other hand decreases selectivity. Therefore, a careful selection of an appropriate reaction temperature is important for a proper yield and a desired selectivity.

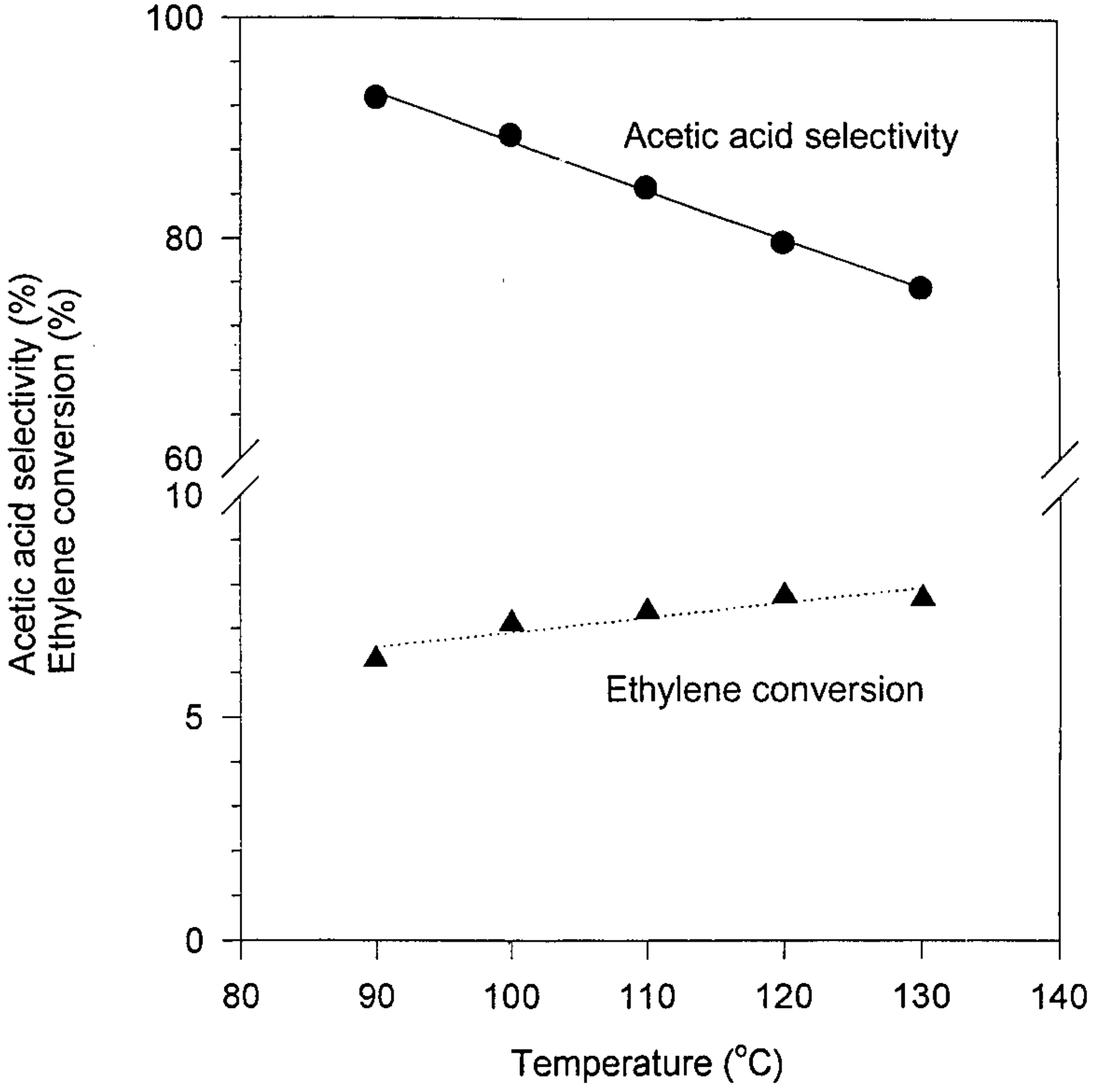

Figure 5.3 Effect of temperature on catalyst activity

5.5 Effect of Pressure

The effect of pressure was examined by conducting the experiments at three different pressures: 120 psig (0.93 MPa), 160 psig (1.2 MPa), and 200 psig (1.4 MPa). Each experimental run had a feed composition of 75 % ethylene. Ten percent palladium supported on HayeSep D was used as the catalyst. The test runs were conducted at three temperatures: 90 °C, 110 °C, and 130 °C.

The results of the effect of pressure on conversion and selectivity are shown in Figure 5.4. It can be seen that both the conversion and selectivity increased linearly with pressure. Such a trend for conversion is expected as the residence time for reactants in the solution is prolonged as the operating pressure is increased. High pressure may also increase gas solubility in liquid. Therefore, ethylene conversion increased as pressure was increased.

Selectivity was also found to increase with increasing operating pressure. It may suggest that the increase in pressure affects the contact between the reactant and the catalyst active surface. Pressure also affects the size of the gas bubbles. However, the actual reason for the increase in selectivity is not known. More studies are required to understand the behavior.

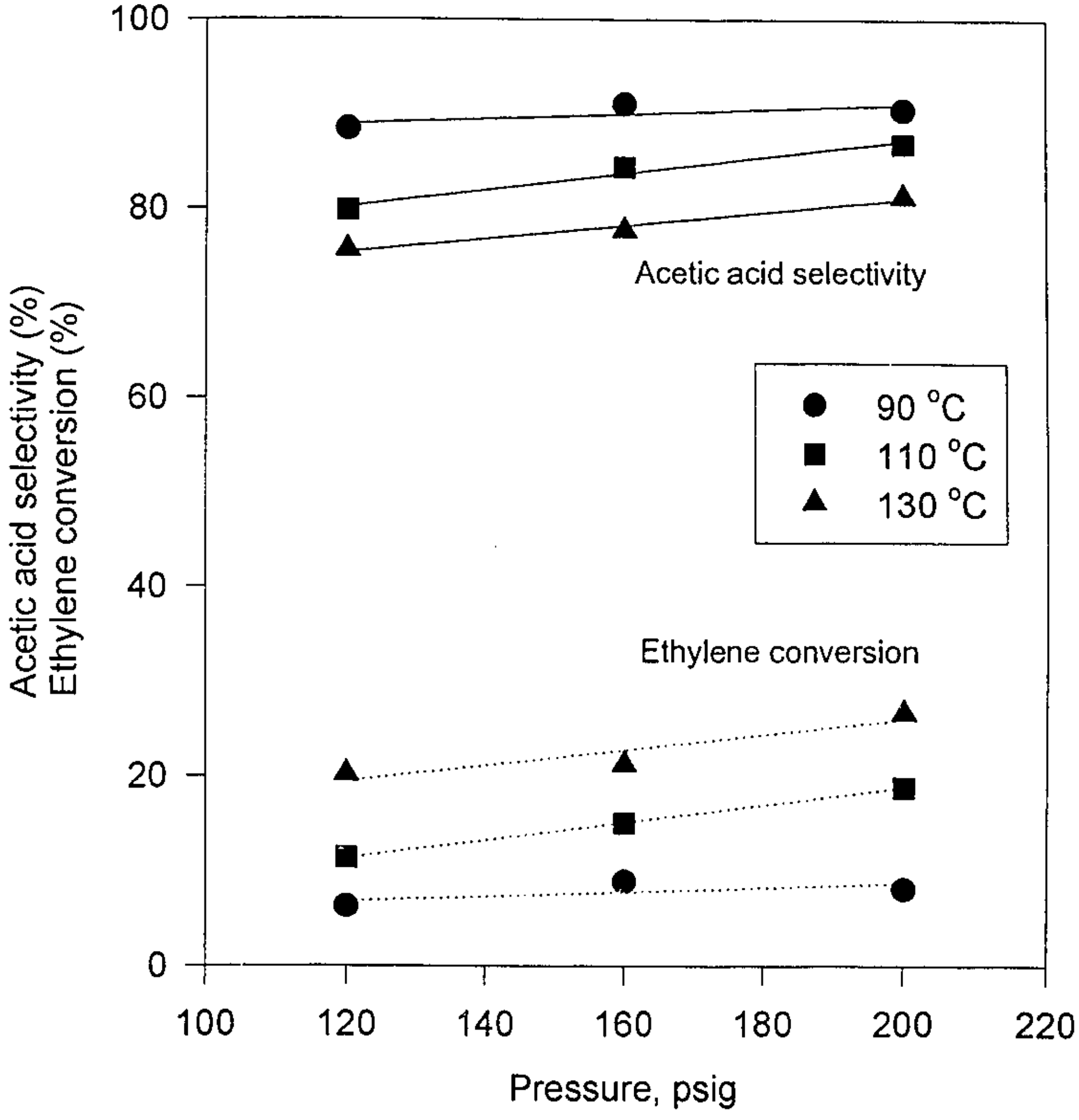

Figure 5.4 Effect of Pressure on Catalyst Activity

5.6 Effect of Additives

Catalyst additives play an important role in many catalyzed reactions. In the Showa Denko process, oxides such as TeO_2 and SeO_2 were added to the catalyst and found to improve the selectivity of the reaction by interacting with the palladium active sites. Therefore, 0.1g of the same additives were dissolved separately into the aqueous phase to see if they affected the catalyst activity. Besides the oxides, NaF was also tested for its effectiveness as a catalyst additive. The comparison of these test results with a test using similar operating conditions but without the additive is given in the following tables. The operating conditions used for the tests listed in Table 5.6 and 5.7 were different. As seen from the tables, the additives showed no significant improvement on the conversion and selectivity of the catalyst.

Table 5.6 Effect of oxides on catalyst activity

Additive	Yield (g CH_3COOH/gPd-h)	Acetic Acid Selectivity (%)
Nil	0.93	89
TeO_2	0.92	89
SeO_2	0.96	85

Table 5.7 Effect of NaF on catalyst activity

Additive	Yield (g CH_3COOH/gPd-h)	Acetic Acid Selectivity (%)
Nil	0.31	82
NaF	0.28	87

5.7 Effect of Feed Composition

One of the factors that will affect the chemistry of a reaction is the feed composition. For the purpose of this study, feed composition was varied from 75 % ethylene to 95 % ethylene, or in terms of ethylene to oxygen ratios: from 5:1 to 11:1. All other reaction parameters such as total flow rate, temperature, and pressure were kept constant. Shown in Figures 5.5 is the effects of feed composition on ethylene conversion and selectivity at 90°C and 130°C. The figure shows that ethylene conversion decreased as the feed composition was richer in ethylene. It may suggest that less oxygen was adsorbed on the catalyst surface as oxygen concentration dropped in the feed. As a result, less chance for adsorbed ethylene to react. Hence, ethylene conversion dropped. Selectivity also decreases with an increase of ethylene concentration in the feed. A similar selective trend was displayed for both temperatures as the ethylene concentration increased in the feed gas. The reason behind the trend of this relationship is not known and further studies are required to understand the behavior.

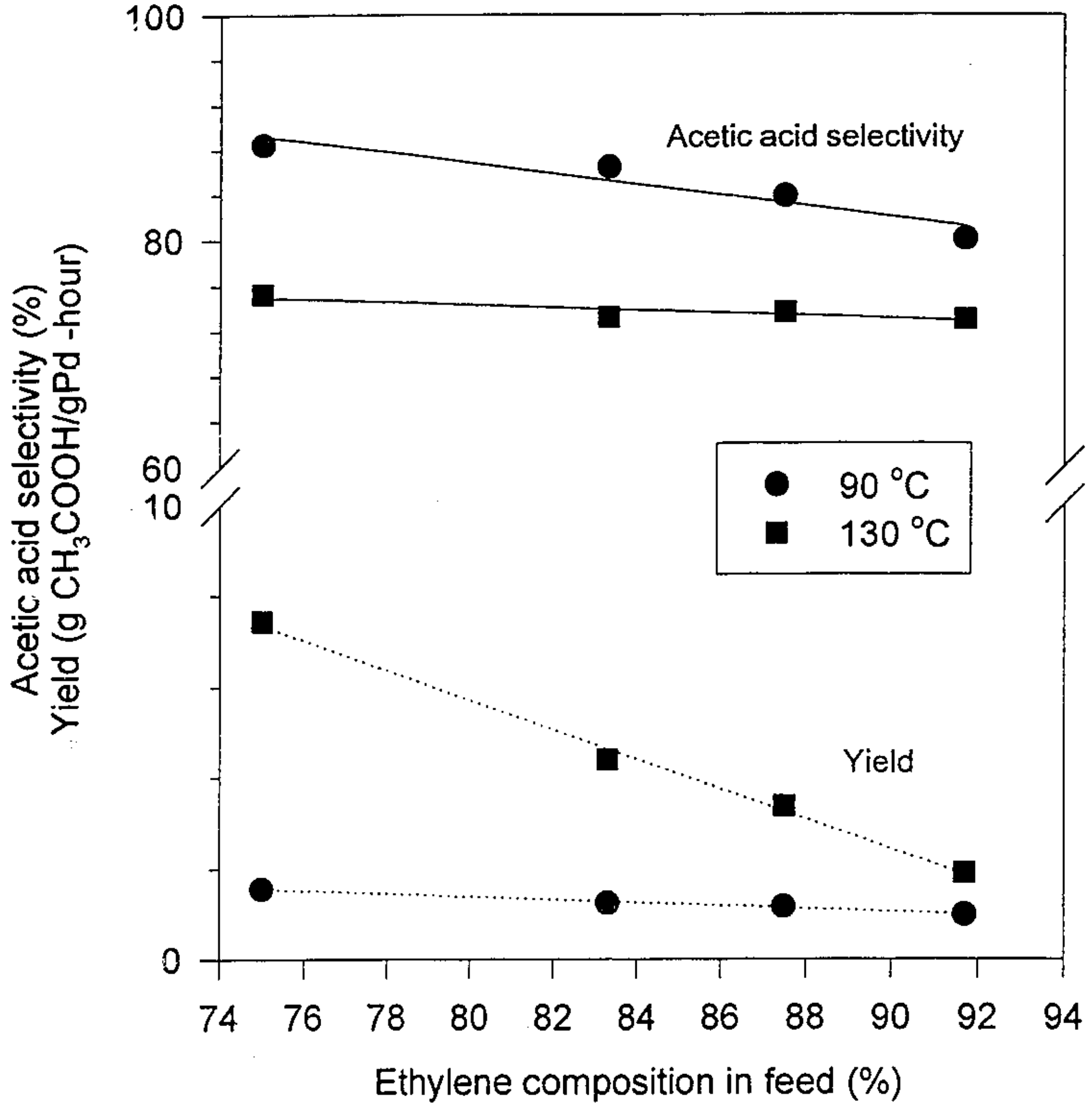

Figure 5.5 Effect of feed composition on catalyst activity

Chapter 6

Mechanism and Kinetics

This chapter will outline the proposed mechanism of ethylene oxidation. Kinetic data were analyzed and overall activation energies were estimated.

6.1 The Slurry Reactor System

The unique feature of a slurry reactor is the suspension of small particles (~100 microns) of catalyst in a liquid phase. In a three phase system, gas bubbles rise through the agitated slurry. There is little relative movement between particles and fluid, even though the liquid is agitated mechanically. The particles tend to move with the liquid. The small particle size, low diffusivities in liquid, and low relative velocity can significantly reduce the overall rate. Hence, mass transport phenomena are important in understanding three phase slurry reactor systems (Smith, 1981).

Presumably, there are two possible modes of transportation by which the reactants reach the catalyst surface. The first involves the transfer of the reactants directly from the gas phase onto the surface of the solid catalyst. The second constitutes the gas-liquid-solid route. Butler (1980) showed photographs of hydrophobic catalyst (Pt-C-Teflon) immersed in water and in alcohol. A silvery sheen on the surface of the catalyst spheres resulting from air trapped between the surface of the catalyst and the water was shown by the catalyst in water. The catalyst surfaces were not wetted due to the hydrophobicity of the catalysts. In contrast, the sample in alcohol appears jet black, and no air sack is observed because the lower surface tension of the alcohol allows complete wetting of the catalyst. Therefore, for catalysts supported on hydrophobic material, gaseous reactants would contact the catalyst surface directly when the catalyst is in water solution.

Shown in Figure 6.1 is the process flow diagram of the three-phase slurry reactor system used in this study. The reactor operated continuously as a steady-flow system with respect to gas phase and as a batch system with respect to the liquid phase.

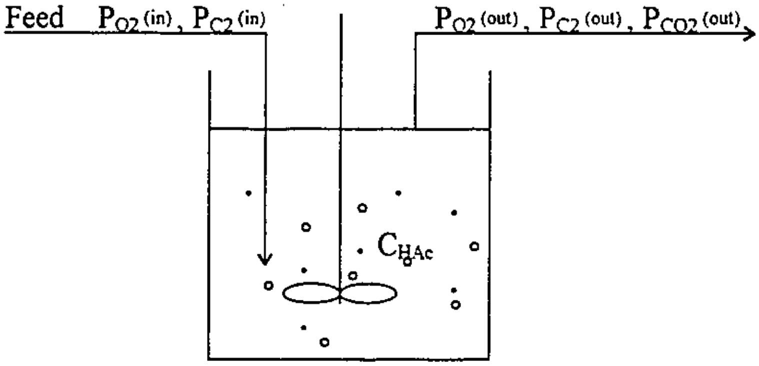

Figure 6.1 The Slurry Reactor System

6.2 Adsorption on Palladium

Golodets (1983) proposed that an adsorbed oxygen atom reacts catalytically with gaseous ethylene. The formation of an "one-point"-adsorption intermediate is then followed by the rupture of a C-C bond in ethylene. The intermediate is proposed to be of the form:

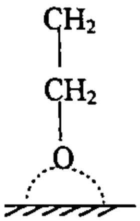

However, Lyons (1988) proposed that both reactants, oxygen and ethylene, were adsorbed on the active centers. Since oxygen and ethylene are highly electrophilic, it is reasonable to argue that they will be both adsorbed on the active surface of the catalyst shown as follows:

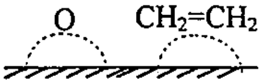

In order for the intermediate proposed by Golodets (1983) to be formed, one species would have a much lower electrophilicity than the other species, but this is not the case for oxygen and ethylene. Furthermore, it was found that the detailed mechanism proposed by Golodets (1983) contradicts itself. Therefore, Lyons' scheme will be adopted in this study and details of a proposed mechanism will be discussed later.

6.3 Development of Kinetic Models

The mechanism of the heterogeneous catalyst oxidation of olefins has been discussed in the literature (Golodets, 1983; Lyons, 1988). In the early stage of this research, the following closed loop network is assumed to be the reaction paths for the irreversible oxidation of ethylene over palladium.

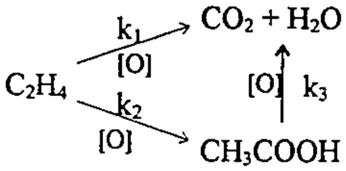
(6.1)

However, it was proposed by Kemball and Patterson (1962) that complete oxidation of ethylene was assumed to be the only path for the formation of carbon dioxide. In this study, the possibility of acetic acid being deep oxidized was examined. In order to determine if this route is possible, an experimental run was carried out at 110°C and 120 psig with 80 mol % of acetic acid as the starting solution and oxygen as the only feed gas. Insignificant amount of carbon dioxide was detected in the exit gas. Also, simple models including the complete oxidation of acetic acid were used to fit the experimental data. The rate constants, k_3, were found to be extremely small in magnitude using linear regression when kinetic data of various temperatures were fitted into several different models. Therefore, it can be concluded that complete oxidation of acetic acid can be neglected when the kinetics are analyzed.

The oxidation of ethylene can then be expressed as the following (Kemball and Patterson, 1962):

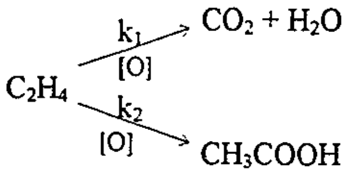
(6.2)

Both of the reactions are irreversible. The mechanism of the oxidation of ethylene will be discussed in more detail. Reaction starts with the electrophilic attack on the adsorbed (CH_2=CH_2) species by the adsorbed oxygen atoms. The reaction mechanism can be written as follows:

step 1: $O_2 + (\ ) \rightarrow (O_2) \rightarrow 2\,(O)$

step 2: $CH_2{=}CH_2 + (\ ) \rightarrow (CH_2{=}CH_2)$

step 3a: $(CH_2{=}CH_2) + (O) \rightarrow (CH_2\text{-}\dot{C}H) + (\dot{O}H)$

step 3b: $(CH_2{=}CH_2) + 3(O) \rightarrow (:CH_2) + (CO_2) + (H_2O) + (\ )$

step 4: $(CH_2\text{-}\dot{C}H) + (O) \rightarrow (CH_3\text{-}\dot{C}{=}O) + (\ )$

step 5:
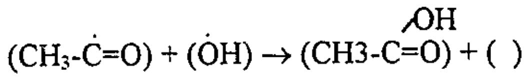
$(CH_3\text{-}\dot{C}{=}O) + (\dot{O}H) \rightarrow (CH3\text{-}\overset{\diagup OH}{C}{=}O) + (\ )$

step 6: $(:CH_2) + 3(O) \rightarrow (CO_2) + (H_2O) + 2(\ )$

where ( ) represents an active site. Steps 1 and 2 are the adsorption of oxygen and ethylene. The initial rupture of one C=C-bond in C_2H_4 is likely to be preferable since its bond energy (264 kJ/mol) is significantly lower than that of the C-H-bond (435 kJ/mol) (Golodets, 1983). Shown in step 3a and 3b are the surface reactions which take place between the adsorbed (O) and (C_2H_4) species. These reactions that causes the breaking of the C=C-bond are the rate-limiting steps. The electrophilic attack gives rise to (CH_2-$\dot{C}H$), an intermediate formed in the partial oxidation of ethylene. For the complete oxidation, three adsorbed oxygen atoms are required in the formation of the species of (:CH_2). That is why the selectivity for carbon dioxide is very much lower compared with that of acetic acid.

There were inadequate experimental data to determine the order for P_{C_2} through curve-fitting. In the development of the rate equation, a simple model was used to fit the experimental data. Recall the parallel reaction paths for the partial and complete oxidation of ethylene:

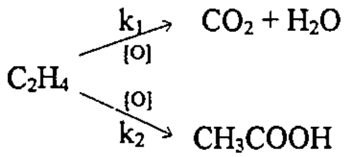

The rate of reaction can be expressed as follows:

$$r_{CO_2} = k_1 \, P_{C_2}{}^{m} \, P_{O_2}{}^{n} \qquad (6.3)$$

$$- r_{C_2} = 0.5 \, k_1 \, P_{C_2}{}^{m} \, P_{O_2}{}^{n} + k_2 \, P_{C_2}{}^{m} \, P_{O_2}{}^{p} \qquad (6.4)$$

The The rate-limiting steps are assumed to be elementary steps. The order for partial pressure of reactants is then related to the number of ethylene molecules and oxygen atoms required for each limiting step. Therefore, m is assumed as unity. Values of 1.5 and 0.5 were used as the order of P_{O_2} for the formation of carbon dioxide and acetic acid respectively. Equation (6.3) and (6.4) becomes:

$$r_{CO_2} = k_1 \, P_{C_2} \, P_{O_2}{}^{1.5} \qquad (6.5)$$

$$- r_{C_2} = 0.5 \, k_1 \, P_{C_2} P_{O_2}{}^{1.5} + k_2 \, P_{C_2} \, P_{O_2}{}^{0.5} \qquad (6.6)$$

where P_{C_2} and P_{O_2} are the partial pressure of ethylene and oxygen respectively and they can be determined as follows:

$$P_i = y_i\,P \tag{6.7}$$

with P being the total pressure and y_i being the molar fraction of species i in the exit gas.

Assuming that the slurry reactor follows the CSTR model, the rate of formation of carbon dioxide and the rate of consumption of ethylene are defined as:

$$r_{CO_2} = \frac{n_{CO_2(out)}}{W} \tag{6.8}$$

$$-r_{C_2} = \frac{n_{C_2\,(in)} - n_{C_2\,(out)}}{W} \tag{6.9}$$

where n_{CO_2} = moles of carbon dioxide

n_{C_2} = moles of ethylene

W = weight of palladium supported on the working catalyst

Using the ideal gas law, number of moles for each gaseous species can be calculated as follows:

$$n_i = \frac{P_i\,V}{RT} \tag{6.10}$$

where R = universal gas constant

V = total gas volume

T = operating temperature

Compiled in Table 6.1 is the kinetic data collected from the experimental runs carried out at various temperatures and feed ratios. The operating pressure for all the kinetics test runs is 120 psig and three different temperatures: 95 °, 100 °, and 120 °C were tested. The feed was 5:1, 7:1, and 9:1 which are the ratios of ethylene to oxygen. All of the kinetic tests were studied at the same impeller speed, 500 rpm, which is close to the optimum speed as determined in section 5.3. The catalyst chosen for this purpose of study is 10 % palladium supported on HayeSep D.

Table 6.1 Experimental data at various temperatures and feed ratios

Feed Ratio (C_2H_4:O_2)	P_{C_2} (out) (Pa)	P_{O_2} (out) (Pa)	P_{CO_2} (out) (Pa)	r_{CO_2} (mol/gPd-s)	$-r_{C_2}$ (mol/gPd-s)
95 °C					
5:1	801396	115348	11981	3.70×10^{-6}	3.34×10^{-5}
7:1	838545	79685	10495	3.38×10^{-6}	2.54×10^{-5}
9:1	860277	59345	9101	3.12×10^{-6}	8.57×10^{-5}
100 °C					
5:1	801953	110611	16160	4.86×10^{-6}	3.98×10^{-5}
7:1	845882	70212	12631	4.05×10^{-6}	2.41×10^{-5}
9:1	865292	51451	11981	3.90×10^{-6}	2.24×10^{-5}
120 °C					
5:1	817556	77827	33341	9.14×10^{-6}	5.70×10^{-5}
7:1	858141	43836	26747	7.81×10^{-6}	4.48×10^{-5}
9:1	874115	32877	21732	7.19×10^{-6}	1.46×10^{-5}

If linear regression is performed on Equation (6.5) and (6.6), k_1 and k_2 are obtained respectively at three different temperatures. Plots of P_{C_2} $P_{O_2}^{1.5}$ against r_{CO_2} and $- r_{C_2}$-

$0.5k_1P_{C_2}P_{O_2}^{1.5}$ versus $P_{C_2}P_{O_2}^{0.5}$ have an average correlation coefficient of 0.96. Listed in Table 6.2 is the values of k_1 and k_2 obtained for different temperatures.

Table 6.2 Rate constants obtained from regression

Temperature (°C)	k_1 (mol/ $Pa^{2.5}$.gPd.s.)	k_2 (mol/ $Pa^{1.5}$.gPd.s)
95	3.01×10^{-20}	3.79×10^{-13}
100	5.16×10^{-20}	2.44×10^{-13}
120	1.50×10^{-19}	5.20×10^{-13}

Using the data from Table 6.2, Arrhenius plots for k_1 and k_2 shown in Figure 6.2 can be made. From the Arrhenius plot, a quantitative evaluation of the apparent activation energies are computed from the slopes, -E/R, obtained by linear regression. These results are summarized in Table 6.3. In the case where mass transfer effects are significant, which could be the case for this reaction, an apparent activation energy would be obtained if the Arrhenius expression is used to compute the activation energy. This apparent value is different from the true activation energy observed in the intrinsic kinetics.

Table 6.3 Apparent Activation Energy

Activation Energy	kJ/mol	Explanation
E_1	74.05	overall activation energy for complete oxidation of ethylene
E_2	23.72	overall activation energy for formation of acetic acid through partial oxidation of ethylene

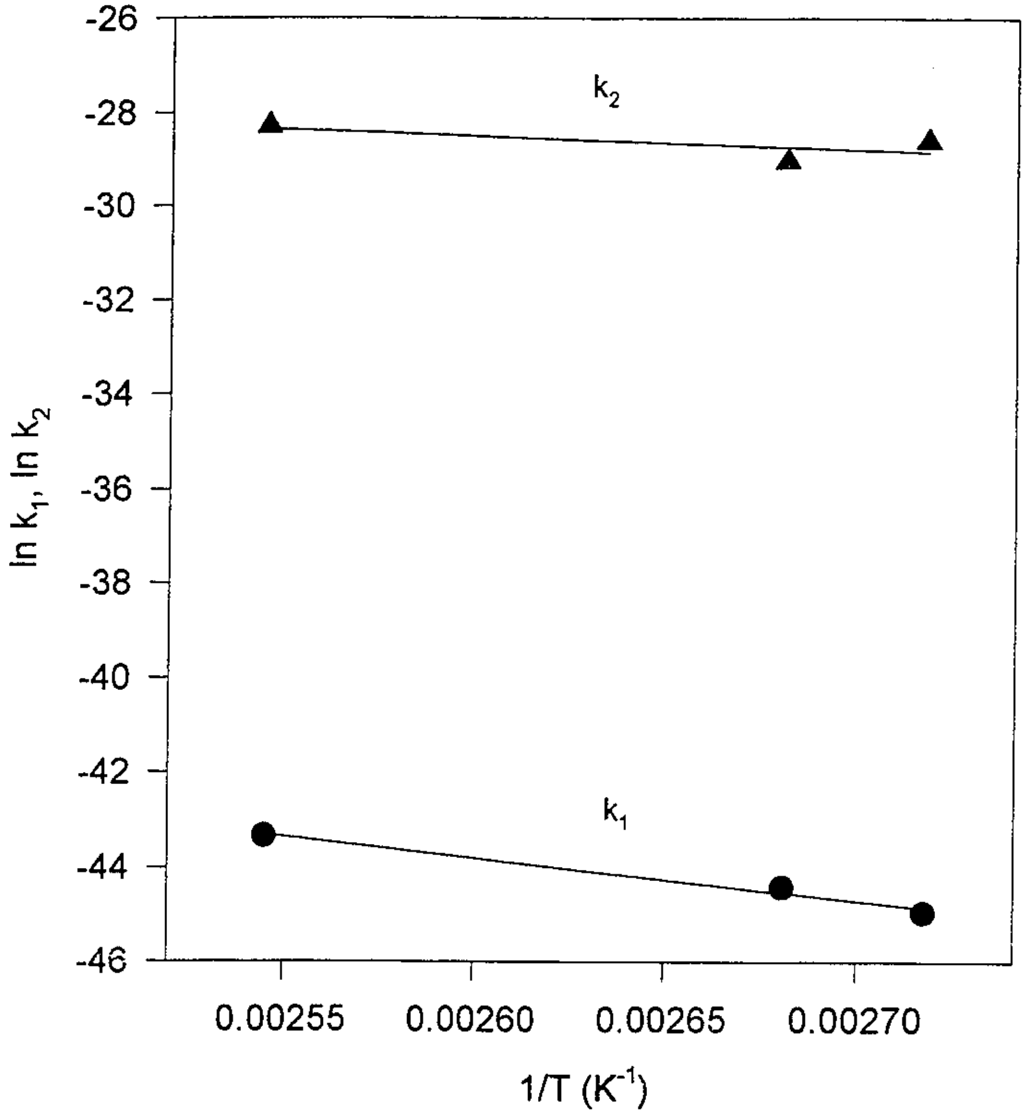

Figure 6.2 Arrhenius plot for k_1 and k_2

The overall activation energy for complete oxidation is about three times higher than that for partial oxidation. This is the reason why the reaction is highly selective. Since the value for E_2 (23.72 kJ/mol), which is overall activation energy for the formation of acetic acid from ethylene, is relatively low for heterogeneous reactions, it may indicate that the kinetic tests were performed within the diffusion regime.

Chapter 7

Conclusions and Recommendation

Hydrophobic catalysts for the one-step oxidation of ethylene to acetic acid were examined in this study. Styrene-divinylbenzene copolymer (SDB), a type of hydrophobic support, displayed a conversion that is twenty times higher than that of hydrophilic carriers such as γ-alumina. Various SDBs and supported metals such as Pd, Pt and Ni were tested. HayeSep D was found to be most effective in the conversion of ethylene to acetic acid. The incorporation of platinum with palladium affected the selectivity by driving the oxidation reaction into completion and forming more carbon dioxide. On the other hand, addition of nickel retarded the activity of the catalyst resulting in a yield of only half the acetic acid amount produced when palladium was used alone. Therefore, it is fair to conclude that palladium by itself was most effective in converting ethylene to acetic acid. Two metal loadings of palladium were compared for their performances and the 10% was found better than the 3% loading.

The effect of operating parameters such as temperature, pressure, additives, impeller speed and feed composition was studied. Increasing the temperature has a favorable effect on ethylene conversion but a deleterious effect on selectivity. Both conversion and selectivity were enhanced by an increase in pressure. Additives such as SeO_2, TeO_2, and

NaF were tested and were found to have no effect on the catalyst activity. Five impeller speeds were tested in order to determine how stirring speed can influence the reaction. The slurry reactor operated at approximately 500 rpm which was the optimum speed. The conversion and selectivity was found to decrease as the impeller speed was increased beyond 750 rpm. Feed composition also affects ethylene conversion and selectivity. Both ethylene conversion and selectivity were lowered as the percentage of ethylene in a feed was increased.

Kinetics for the process was studied and the apparent activation energy for the ethylene oxidation was estimated. Regression on the data for the suggested rate equations yielded activation energies of 74.05 kJ/mol and 23.72 kJ/mol for the complete and partial oxidation of ethylene respectively. Since the apparent activation energy for partial oxidation is relatively low, it may indicate that the kinetic tests were performed within the mass transfer regime.

Although mass flow controllers were used in the experiment, volumetric flow rates of feed gases fluctuated due to the low flow rate used. Results of some test runs were discarded because of the flow rate discrepancy from the set point value. The way the equipment was set up did not allow any moment to moment correction when flow rate was suspected to fluctuate. Therefore, a multiple-way valve is recommended to be installed in the line before it enters the reactor. This modification would allow measurement of inlet flow rates throughout the course of an experimental run and correction of flow rates if necessary.

Vortex effect was encountered at high stirring speed. Presence of vortex affects mass transfer of the reactants and complicates the kinetic study. It is recommended that placing baffles into the reactor may help to prevent the formation of vortex.

With the information obtained from the kinetics examined in this study, a cost study can be made to determine if the commercialization of this process is economically feasible. More research would be required to improve the ethylene conversion and in particular, the selectivity. This can be done by progressively adjusting the composition and preparation of the catalyst. Furthermore, detailed studies on reaction mechanism and kinetic models are also required in order to determine the complex kinetics involved.

Bibliography

Aguilo, A.; Hobbs, C.C.; Zey, E.G., *Ullmann's Encyclopedia of Industrial Chemistry*, 5th ed., vol. A1, VCH Publishers: Deerfield Beach, Florida, 1985; 45-64.

Anderson, J.R.; Pratt, K.C., *"Introduction to Characterization and Testing of Catalysis"*, Academic Press: Sydney, Australia, 1985; Chapter 2.

Butler, J.P., "Hydrogen Isotope Separation by Catalyzed Exchange between Hydrogen and Liquid Water", *Separation Science and Technology*, **1980**, *15(3)*, 371-396.

Chauvin, Y.; Commereuc, D.; and Dawans, F., "Polymer Supported Catalysts", *Prog. Prog. Polym. Sci*, **1977**, *5*, 95-126.

Chuang, K.T.; Fu, L., *U.S. Patent No. 5,210,319*, 1993.

Chuang K.T.; Zhou, B.; Tong, S., "Kinetics and Mechanism of Catalytic Oxidation of Formaldehyde over Hydrophobic Catalysts", *Ind. Eng. Chem. Res.*, **1994**, *33*, 1680-1686.

Chrisope, D.R.; Beak, P., *J. Am. Chem. Soc.*, **1986**, *108*, 334.

Cullity, B.D., *Elements of X-Ray Diffraction*, Addison-Wesley Publishing Co., 1967.

David, R., Estienne, J., *U.S. Patent No. 3,624,147*, 1971.

Fu, L.; Chuang, K.T., "Control of NOx Emissions by Selective Catalytic Reduction with Hydrogen over Hydrophobic Catalysis", *J. Ener. Fuels*, **1989**, *3*, 740-743.

Golodets, G.I., "Heterogeneous Catalytic Reactions Involving Molecular Oxygen", *Studies in Surface Science and Catalysis*, Elsevier Scientific Publishing Company: Amsterdam, 1983; 280-311.

Goncharova, S.N.; Paukshtis, E.A.; Bal'zhinimaev, B.S., "Size effects in ethylene oxidation on silver catalysts. Influence of support and Cs promoter", *Appl. Catal. A: Gen.*, **1995**, *126*, 67-84.

Greene, H.L.; Ramachandran, B; Chatterjee, S., "Selective Osidation Catalysts for Halogenated Organics", *U.S. Patent No. 5,457,268*, 1995.

Henry, P.M., *Palladium Catalyzed Oxidation of Hydrocarbons*, D Riedel Publishing Co.: Dordreche, Holland, 1980; Chapters 1-2.

Hinnenkamp, J. A., *U.S. Patent No. 4,453,598*, 1984.

JCPDS International Centre for Diffraction, "*Powder Diffraction File*", Swarthmore, Pennsylvania, 1989.

Kawakami, K.; Isobe, M.; Horiki, K.; Kusunoki, K., "Kinetic Study of Isotopic Exchange Reaction between Hydrogen and Water Vapor over a Pt/SDBC Hydrophobic Catalyst Sheet", *Can. J. Chem. Eng.*, **1988**, *66*, 338-342.

Kemball, C.; Patterson, W.R., *Proc. Roy. Soc.*, **1962**, *A270*, 219.

Kirk, R.E.; Othmer, D.F., *Encyclopedia of Chemical Technology*, Vol. 1, 4th Ed., John-Wiley and Sons, New York, 1992.

Klugherz, P.D.; Harriott, P., "Kinetics of Ethylene Oxidation on a Supported Silver Catalyst", *AIChE J.*, **1971**, *17(4)*, 856-866.

Kroschwitz, J. I., *Kirk-Othmer Encyclopedia of Chemical Technology*, 4th ed., John Wiley & Sons: New York, 1991: vol 1, 121-138.

Ledjef, K., "Elimination of Hydrogen or Oxygen from Explosive Mixtures by Catalytic Techniques", *Int. J. Hydrogen Ener.*, **1987**, *12*, 361-367.

Lemaitre, J.L.; Menon, P.G.; Delannay, F., "The measurement of Catalyst Dispersion", *Characterization of Heterogeneous Catalysts*, Marcel Dekker Inc.: New York and Basel, 1984; Chapter 7.

Le Page, J.F., *Applied Heterogeneous Catalysis*, Editions Technip: Paris, 1987; Chapters 3 and 5.

Lieto, J.; Milstein, D.; Albright, R.L.; Minkiewicz, J.V.; and Gates, B.C., "Polymeric Supports for Catalysis", *J. CHEMTECH*, **1983**, 46-53.

Lloyd D. I.; Eve, P.L.; Gammer, D.P., "A Comparison of Naphtha Oxidation and Catalyzed Low Pressure Methanol Carbonylation for the Production of Acetic Acid", *Erdoel Erdgas Kohle*, **1993**, *109 (6)*, 266-269.

Lyons, J.E., "Selective Oxidation of Hydrocarbons via C-H Bond Activation by Soluble and Supported Palladium Catalysis", *Catal. Today*, **1988**, *3(2)*, 245-258.

Patterson, W.R.; Kemball, C., *J. Catal.* **1963**, *2*, 465.

Perry, R.H.; Green, D., *Perry's Chemical Engineers' Handbook*, 6th ed., McGraw-Hill Publisher: New York, 1984; 4-46.

Seiyama, T.; Aramaki, M.; Takeyama, N.; and Yamazoe, N., *Kogyo Kagaku Zasshi*, **1971**, *74*, 672.

Seiyama, T.; Yamazoe, N.; Hojo, J.; Hayakawa, M., "Catalytic Oxidation of Olefins over Metallic Palladium Suspended in Water", *J. Catal.*, **1972**, *124*, 173-177.

Sherwood, A.E., "Kinetics of Catalyzed Oxidation in Air at Ambient Temperature", *Am. Chem. Soc. Natl. Top. Meet.*, Dayton, Ohio, April 1981.

Shyamal K.B.; Musti, S.R., "Selective Oxidation of n-Butane to Maleic Anhydride. 3. Modeling Studies", *Ind. Eng. Chem. Res.*, **1991**, *30*, 1829-1832.

Smith, J.M., *Chemical Engineering Kinetics*, 3rd ed., McGraw-Hill: New York, 1981; Chapter 5.

Sood, S., One-step Oxidation of Propylene to Acetic Acid. M.Sc. Thesis, University of Alberta, Edmonton, Canada, 1995.

Stern, E.W., *Catal. Rev.*, **1968**, *1*, 73-152.

Stolyarov, I.P.; Varfaftik, M.N.; Nefedov O.M.; Moiseev, I. I., *Kinetika i Kataliz*, **1982**, *23*, 376.

Suzuki, T.; Yoshikawa, H.; Abe, K.; Sano, K., "Process for producing acetic acid", *European Patent No. 620,205 A1*, 1994.

Swodenk, W.; Scharfe, G., *U.S. Patent No. 3,925,452*, 1975.

Trost, B.M.; Metzner, P.J., *J. Am. Chem. Soc.*, **1980**, *102*, 3572.

Yaparpalvi, R.; Chuang, K.T., "Fluorinated Styrene Divinylbenzene Copolymer as Catalyst Support", *Appl. Catal.*, **1991**, *72*, 71-80.